DEVELOPING ARTIFICIAL CORNEAL ENDOTHELIUM MICRO-ENVIRONMENT USING BIOINSPIRED APPROACH

by

Fatma Zehra Erkoç

B.S., Bioengineering, Yıldız Technical University, 2013

Submitted to the Institute of Biomedical Engineering
in partial fulfillment of the requirements
for the degree of
Master of Science
in
Biomedical Engineering

Boğaziçi University
2017

DEVELOPING ARTIFICIAL CORNEAL ENDOTHELIUM MICRO-ENVIRONMENT USING BIOINSPIRED APPROACH

APPROVED BY:

Assoc. Prof. Dr. Bora Garipcan .....
(Thesis Advisor)

Assoc. Prof. Dr. Albert Güveniş .....

Assist. Prof. Dr. Sedat Odabaş .....

DATE OF APPROVAL: 9 January 2017

ACKNOWLEDGEMENTS

Firstly, I would like to express my immeasurable appreciation and utmost gratitude to my thesis advisor, Assoc. Prof. Dr. Bora Garipcan, for his endless support and encouragement throughout this project. His guidance along with unwavering scientific and moral support has helped me bring this study into success.

In addition, I would like to thank my thesis committee: Assoc. Prof. Dr. Albert Güveniş, and Assist. Prof. Dr. Sedat Odabaş for their valuable comments. I would also like to thank Assist. Prof. Dr. Ayşe Ak for her invaluable efforts in my education.

I would also like to thank Bogaziçi University Scientific Research Fund (BAP) for their support under Grant Number No.11501 along with TÜBİTAK 2210-C Program of Domestic Graduate Scholarship in Priority Areas for their support.

I am truly thankful to my team mate, Alp Özgün, for his boundless assist and moral support in every stages of this project. Special thanks to my friends Sabra Rostami, Hilay Şencan, Özgen Öztürk, Sezin Eren, Ecem Sahin, Fatih Puza, Berkay Erenay, all my laboratory colleagues and my dearest friends Deniz Çınar, Celal Biradlı, Hatice Kaya, and Seher Dağtekin for their long lasting friendship.

Lastly, I am deeply appreciative to my family who have always believed in me and gave their unconditional love. I am dedicating my thesis to my father who has always have faith in me to become a successful scientist.

ACADEMIC ETHICS AND INTEGRITY STATEMENT

I, Fatma Zehra Erkoç, hereby certify that I am aware of the Academic Ethics and Integrity Policy issued by the Council of Higher Education (YÖK) and I fully acknowledge all the consequences due to its violation by plagiarism or any other way.

Name :

Signature:

Date:

ABSTRACT

DEVELOPING ARTIFICIAL CORNEAL ENDOTHELIUM MICRO-ENVIRONMENT USING BIOINSPIRED APPROACH

In this thesis, micro-environment of healthy corneal endothelium was prepared by mimicking the stiffness and chemistry of underlying layer of endothelium, and inspiring from topography of corneal endothelium. Polyacrylamide (PAAm) hydrogel cell substrates were synthesized with in the stiffness range of Descemet's membrane's elastic modulus value of 20-80 kPa. Hexagonal patterns with dimensions 20μm in diameter and 4μm in depth which inspired from mostly hexagonally shaped corneal endothelial cells (CECs) were created on silicon wafer mold via photolithography and transferred to PAAm hydrogels by using soft lithography technique. PAAm hydrogels which have hexagonal patterns were modified with Collagen IV (Col IV), hyaluronic acid (HA) and different amount mixtures of Col IV and HA to mimic corneal endothelium biochemically as well. Chemical modifications were confirmed with Fourier Transform Infrared Spectroscopy (FTIR), Water Contact Angle (WCA) Measurements and Immunofluorescence imaging. After characterization, adhesion, viability and morphology of corneal endothelial cells on these substrates were investigated. The results of cell culture studies indicate that surface topography of substrates enhances cell viability significantly while altering cell morphology. Moreover chemical composition of substrate surface was shown to be an important parameter for growing cell sheets. These results provide a proof of concept for biomimetic and bioinspired strategies for corneal recovery through clinical translations of cell sheet growth approaches.

Keywords: Corneal endothelium, bioinspired, polyacrylamide, hydrogel, topography, micro-environment.

ÖZET

BİYOESİNLENME YAKLAŞIMIYLA YAPAY KORNEA ENDOTELYUM MİKRO-ÇEVRESİNİN GELİŞTİRİLMESİ

Bu tez çalışmasında, kornea endotelyumun altında bulunan tabakanın sertliği ve kimyasal yapısı taklit edilerek ve endotelyumun topografisinden esinlenilerek sağlıklı kornea endotelyumu mikroçevresi hazırlanmıştır.Descemet membranın 20 ila 80 kPa sertlik aralığında poliakrilamid hücre substratları sentezlenmiştir. Kornea endotelyum hücrelerinin çoğunlukla altıgen olan 20μm çapında ve 4μm derinliğinde şekillerinden esinlenilerek silikon kalıplar üzerinde fotolitografi tekniğiyle altıgen desenler oluşturulmuş ve bu desenler yumuşak litografi yöntemiyle substratlara aktarılmıştır. Üzerlerinde altıgen desenler bulunan PAAm hidrojeller endotelyumun mikroçevresini biyokimyasal olarak da taklit edebilmek için tip 4 kolajen, hyaluronik asit, tip 4 kolajen ve hyaluronik asit karışımlarının farklı oranlarıyla modifiye edilmiştir. Kimyasal modifikasyonlar Fourier Dönüşümlü Infrared Spektrofotometre (FTIR), Su Temas Açısı Ölçümleri (WCA) ve Immunofloresans görüntüleme yöntemleriyle doğrulanmıştır. Karakterizasyon aşamasından sonra, kornea endotelyum hücrelerinin hazırlanan bu substratlar üzerinde tutunması, canlılığı ve morfolojileri incelenmiştir. Hücre kültürü çalışmalarının sonuçları substratların yüzey topografilerinin hücre morfolojisini değiştirmekle birlikte canlılığı önemli ölçüde arttırdığını göstermiştir. Buna ek olarak, substrat yüzeyinin kimyasal bileşiminin hücre tabakası oluşturulmasında önemli bir parametre olduğu gösterilmiştir. Bu sonuçlar, kornea iyileştirilmesinde hücre tabakalarının klinik uygulamalarında biyotaklit ve biyoesinlenmiş stratejilerin kullanılabileceğini göstermektedir.

Anahtar Sözcükler: Kornea endotelyum, biyoesinlenmiş, poliakrilamid, hidrojel, topografi, mikro-çevre.

TABLE OF CONTENTS

LIST OF FIGURES

LIST OF TABLES

LIST OF SYMBOLS

E	Young's Modulus
G'	Storage Modulus
G"	Loss Modulus

LIST OF ABBREVIATIONS

APS	Ammonium Persulfate
APTES	3-aminopropyltrimethoxysilane
Col IV	Collagen Type IV
BCECs	Bovine Corneal Endothelial Cells
CECs	Corneal Endothelial Cells
DMEM	Dulbecco's Modified Eagle's Medium
DMSO	Dimethyl Sulfoxide
ECM	Extracellular Matrix
FBS	Fetal Bovine Serum
FTIR	Fourier Transform Infrared Spectroscopy
HA	Hyaluronic Acid
HCECs	Human Corneal Endothelial Cells
MTT	3-[4, 5-Dimethylthiazol-2-Yl]-2, 5 Diphenyltetrazolium Bromide
OD	Optical Density
PAAm	Polyacrylamide
PBS	Phosphate Buffered Saline
RT	Room Temperature
Sulfo-SANPAH	Sulfosuccinimidyl-6-(40-azido-20-nitrophenylamino) Hexanoate
TCP	Tissue Culture Plate
TEMED	Tetramethylethylenediamine
WCA	Water Contact Angle

1. INTRODUCTION

1.1 Motivation

Corneal endothelium is the innermost layer of cornea which has five histologically different layers and composed of mostly hexagonally shaped corneal endothelial cells' (CECs) monolayer. Corneal endothelium has important functions such as retaining corneal transparency, serving as a pump to provide hydration and being a leaky barrier for fluid and metabolic substances [1].

Corneal endothelial cells have high metabolic activity, but they do not divide in vivo. So, corneal endothelial cells decrease in number as age progresses and thus become larger to make up for the lost space. Diseases that cause loss of cells in the cornea also cause this effect resulting in decreased clarity of cornea, blurred vision and blindness in severe cases [2, 3]. Replacement of cornea is clinically applied in mainly two ways, transplantation from donors or keratoprosthesis. Both of these approaches come with considerable caveats. Since no biomaterial is flawless in every way, immune reactions against the material will arise in some cases no matter how good the design is [4].

Cell therapy is a promising approach in replacing lost corneal tissue. Lots of tissue engineering approaches show effort to generate corneal tissue using different types of stem cells and biomaterials [5]. As an example, Koo, et al tested different topographies on polydimethylsiloxane (PDMS) with several extracellular matrix protein coatings and concluded that topographical and biochemical characteristics can enhance the morphometry and phenotype of human corneal endothelial cells(HCECs) [6]. In another study, Palchesko, et al prepared PDMS substrate with different elastic modulus and different ECM protein coatings and investigate the behavior of bovine corneal endothelial cell on these substrates. Among thirty six different conditions, Col IV coated PDMS substrate which has 50 kPa elastic modulus shows the best phenotypic

expression of ZO-1 [7].

Our approach is to create a cell sheet for corneal recovery while retaining natural morphology and chemical composition of ECM with the inspiration of these studies. Using patterns inspired from in vivo morphologies of corneal endothelial cells will provide a proof of concept for enhancing the outcome of cell sheet strategies and increasing the chance for translation into clinical applications.

1.2 Objectives

In this thesis, developing artificial corneal endothelium micro-environment using bioinspired approach was aimed. To this end, polyacrylamide hydrogels with elastic modulus of approximately 50 kPa were prepared to mimic the stiffness of Descemet's membrane of the human cornea. Afterwards soft lithography technique was used to produce hexagonal-shaped micro-patterns on hydrogels so as to mimic corneal endothelial cells' topographical features. After this stage, prepared hydrogels were modified with collagen IV and hyaluronic acid to mimic biochemistry of corneal endothelial cell micro-environment.

The main objectives of this study are as follows:

- To prepare and characterize polyacrylamide hydrogels
- To mimic Descemet's membrane's stiffness,
- To fabricate bioinspired hydrogels with hexagonal-shaped micro-topography having desired stiffness and chemical compositions,
- To investigate behavior of bovine corneal endothelial cells on these prepared substrates.

1.3 Outline

The presentation of the thesis is as follows. Chapter 2 contains background information regarding structure and functions of human cornea, the corneal endothelium, recovery strategies of corneal endothelium, artificial corneal endothelium and bioinspired approaches to corneal recovery. In chapter 3, experimental details are described. After experimental procedures, results are given in chapter 4. Finally, discussions of obtained results and future works are introduced in chapter 5.

2. BACKGROUND

2.1 Cornea: Structure and Functions

The human cornea is an avascular and transparent connective tissue with approximate horizontal diameter of 11.5 mm and vertical diameter of 10.5 mm in typical fully grown people. Besides posing as structural and infection barrier for the eye, cornea is also in charge of refractive functions of the eye [8, 9]. The human cornea contains many layers which are different from each other histologically. These layers are the epithelium, the anterior basement membrane, Bowman's layer, the stroma, Descemet's membrane (posterior basement membrane) and the endothelium respectively [10]. Each layer has its own unique structure and function. Figure 2.1 is a schematic representation of human cornea layers.

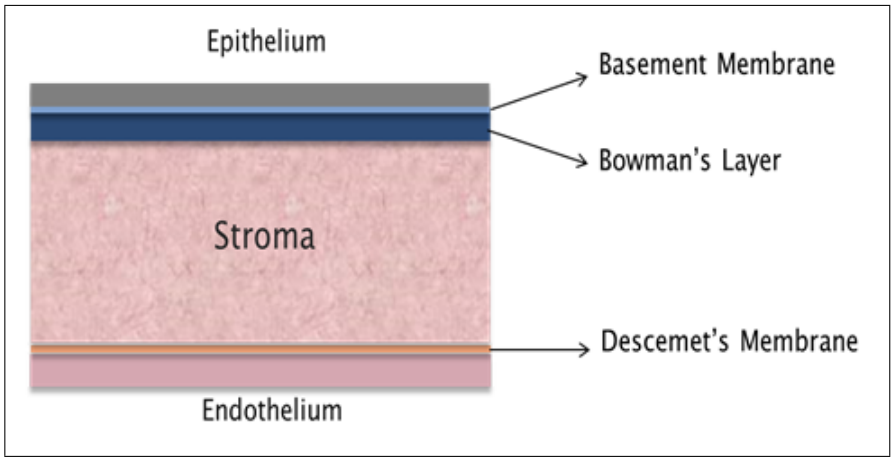

Figure 2.1 Layers of cornea (redrafted from [10, 11]).

Epithelium is the outermost layer of cornea which provides the first line of defense against outside pathogens. It also plays a vital role in refractive function of the cornea. Corneal epithelium is formed by four to six layers of nonkeratinized, stratified squamous epithelial cells and its thickness is about 40-50 4μm. The most outer two to three layers which have flat and polygonal shape have apical microvilli

and microplicae. These layers are also coated with a charged glycocalyx which is important for the adjustment of surface area between the tear film's mucinous layer and the cell membrane. These external cell layers act as barriers which prevent toxins and microorganisms from penetrating deeper layers of cornea with the help of tight junctions [8, 9]. Basal epithelial cell layer, the inmost layer of the corneal epithelium, is a single layer of cells with a length of approximately 20 μm. These cells have capability of mitosis in addition to their other important function which is attaching to the underlying basement membrane with a hemidesmosomal system. This powerful attachment provides integrity with the other underlying corneal layers [9].

The epithelial basement membrane is located between basal epithelial cells and stroma. Basement membranes are thin acellular layers which are placed under the cells and have function in adhere them to their interstitial matrix and also disconnect them from their interstitial matrix. In addition to having function in connecting adjacent cells, they serve also in related epithelial or endothelial cells' migration, differentiation, and prolongation of the differentiated phenotype of these cells by adjusting local concentrations of cytokines and growth factors. The epithelial basement membrane consists of various extracellular molecules such as collagens, laminins, heparan sulfate proteoglycans, and nidogens. It has critical function in sustaining corneal homeostasis and corneal wound healing [12].

Bowman's layer which is placed between the epithelial basement membrane and stroma, is an acellular layer which of depth is nearly 8-12 μm and its thickness gets thinner in progress of time. Its collagen fibrils are united with anterior stroma and they constitute the thickness that half to two-thirds the thickness of collagen fibrils in the stroma. Bowman's layer may protect the subepithelial nerve plexus which arriving from the anterior stroma. However, it has no crucial function for corneal physiology. Some diseases such as advanced bullous keratopathy cause the destruction of Bowman's layer but this situation does not bring about loss of vision or structural changes of whole cornea [8, 13].

The corneal stroma constitutes approximately 80% to 85% of corneal thickness

by having 500 μm thickness in human. This layer is formed by the network structure of collagen fibers, ground substance and extracellular matrix components such as water, inorganic salts, proteoglycans and glycoproteins. Heterodimeric complex of Type I and Type V collagen composes stromal collagen fibrils which have narrow diameter. Stromal collagen fibers are organized as parallel bundles and these bundles are piled as parallel layers which called lamellae. The stroma is highly organized network structure which has 200 to 250 distinctive lamella. This proper organization of stromal fibers and ECM provides transparency and mechanical endurance to stroma. The major cell type of the stroma is keratocyte. These cells can synthesis collagen molecules, glycosaminoglycans and matrix metalloproteases (MMPs) to continue stromal homeostasis [8, 9]. The concentration of proteoglycans and patterns of collagen lamellae change with depth throughout the stroma. Because of this difference in concentration of proteoglycans, greater hydration occurs in the posterior stroma. The refractive index of the cornea goes down, while light passes through the anterior-posterior axis due to a more hydrated posterior cornea. Transparency is provided by this way. Lastly, stroma also plays a critical role in corneal immunity. Epithelium is responsible for surface immune regulation, in addition to this immature and precursor-type dendritic cells are placed in central cornea and resident bone marrow-derived dendritic cells are seen in peripheral cornea. However, macrophages are located in the posterior stroma [8].

Descemet's membrane is the underlying membrane of the corneal endothelium and its thickness is around 3 mm in children, gradually becomes thick to 10 μm in adults because of the secretion collagen by endothelial cells [3, 8]. This membrane is formed by two layers: an anterior banded layer and a posterior nonbanded layer. The former one is composed of collagen lamellae and proteoglycans, latter is placed under the endothelial cells and becomes thick over the years. Descemet membrane includes collagen type IV and VIII fibrils. Other basement membranes throughout the body also contains collagen type IV but collagen type VIII is comparatively particular to Descemet membrane and it can be seen under electron microscopy as ladder-like structures. When it comes to function of Descemet's membrane, it helps to sustenance of corneal dehydration. If iatrogenic Descemet membrane tear or detachment occurs following the intraocular surgery, corneal edema develops [8].

2.2 The Corneal Endothelium

The corneal endothelium is formed by the single layer of mostly hexagonally shaped corneal endothelial cells and it locates between the corneal stroma and anterior chamber. The corneal endothelium has crucial function in sustaining corneal transparency via controlling corneal hydration [1]. Optical transparency of this tissue is provided by crystalline organization and significant distance of collagen fibrils. Since piling up any fluid would disturb transparency, the corneal endothelium serves as a barrier and pump. Endothelium allows the transition of nutrients and other molecules from the aqueous humor into the avascular cornea [1, 3]. In addition to being leaky barrier for fluid and metabolic substances, endothelium acts also as an active pump which carry ions and draw water through osmosis from the stroma into the aqueous humor [3]. The corneal endothelial cells have high metabolic activity since they have plentiful mitochondria, rough and smooth endoplasmic reticulum and Golgi apparatus [1]. However, these cells do not proliferate in vivo. For instance, a month later the birth, human endothelial cell density is around 6000 cell/mm^2. This rate decreases to nearly 3500 cell/mm^2 after five years. When age comes 85, endothelial cell density goes down 2300 cell/mm^2, whereas this rate is approximately 3400 cell/mm^2 at the age of 15 [3]. Despite the decrease in the number of the endothelial cells, the corneal endothelium can keep corneal transparency unless the endothelial cell density falls behind the critical level which is generally 400-500 cells/mm^2 [14].

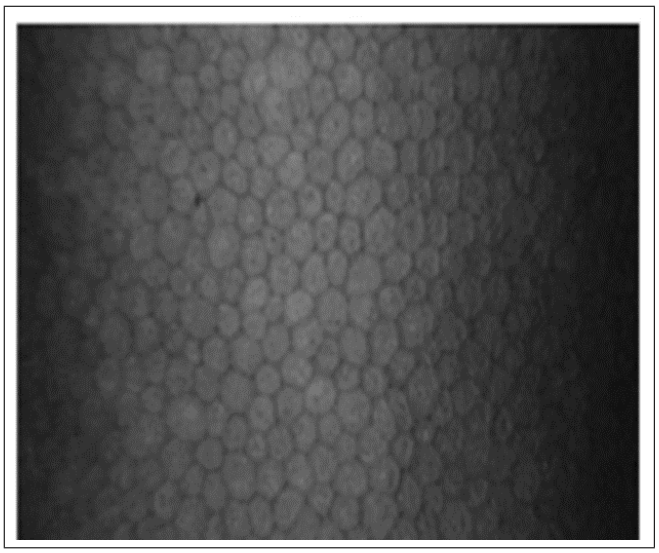

Figure 2.2 Corneal confocal microscopy image of the human corneal endothelium [15].

There are several reasons which can contribute to damage of corneal endothelium such as inflammation in the eye, very high intraocular pressure, surgical trauma which in most cases results in corneal edema, and endothelial dystrophies which include Fuchs' dystrophy, Posterior polymorphous dystrophy (PPD), Congenital hereditary endothelial dystrophy (CHED), Iridocorneal endothelial syndrome (ICE), Intermediate forms. Wearing contact lenses can also bring about some changes on corneal endothelium in the long term [3, 8, 16]. As an example, Fuchs' dystrophy is the most prevalent and hereditary disease which endothelial cells decreased faster, rest living cells enlarge their size of and secrete large amount of improper banded Descemet's membrane and finally cause the disease which is known as a cornea guttata. At this situation, endothelium fails in performing pump and barrier function and cannot preserve its transparency [3]. As result of thickening Descemet's membrane and changing corneal endothelial cells' size and shape, the cornea gradually becomes like opaque. This situation creates blurry vision. Injuring corneal endothelium due to any reasons is probably more severe than that to the other layers of cornea, since the corneal endothelium cell loss isn't reversible and eventually affects visual function [2].

2.3 Recovery Strategies of Corneal Endothelium

The main treatment for the recovery of cornea is transplantation which is called as also keratoplasty. There are two types of keratoplasty, namely penetrating kerotoplasty and lamellar keratoplasty. The former is an operation which includes full-thickness replacement of the cornea and the latter is altering only unhealthy layers of cornea. When compare to each other, studies have shown that lamellar keratoplasty which includes anterior lamellar keratoplasty and endothelial keratoplasty techniques ends up with improved visual outcomes and reduced complication [17, 18]. Descemet's stripping automated endothelial keratoplasty (DSAEK) is most common technique for the corneal endothelial cells dysfunction. In USA, the years between 2005 and 2010, applying endothelial keratoplasty increased exponentially and it became most widely used technique [19]. Nevertheless, there are still some challenges in endothelial keratoplasty such as donor shortage, problems which are related with surgical procedures, postoperative cell loss, and raising in generation glaucoma after operation [2, 19]. Most importantly to solve donor tissue shortage problem, several approaches are developed.

These are cell therapy, using stem cells, artificial or bioengineered corneas, and gene therapy [5]. One approach is also that using Rho-kinase (ROCK) inhibitor namely Y-27632 to decelerate endothelial cell degeneration and prevent apoptosis. One study shows that ROCK inhibitor Y-27632 encourages cynomolgus monkeyderived MCECs' proliferation [20]. In cell therapy approach, three main cell types are used such as corneal endothelial progenitors, stem cell-derived corneal endothelial cells (CECs), and human corneal endothelial cells (HCECs) which are isolated and purified from a cadaveric donor cornea [21]. While cells can be directly injected into the anterior chamber of the eye, three dimensional cell substrates are also designed and tried for obtaining transplantable cell sheets [5, 22]. As another approach Moysidis et al. (2015) have used magnetic nanoparticles to enhance delivery and efficiency of cell therapy. This approach did not bring about any change in the viability or identity of the HCECs and enhance the efficiency of cell delivery in vitro [23].

When it comes to tissue engineered corneal endothelium, lots of substrates were

designed to culture human corneal endothelial cells (HCECs) in vitro. These cell substrates are formed by biological, synthetic and biosynthetic materials. As biological substrates, denuded amniotic membranes, de-cellularized corneal layers, and de-epithelialized human anterior lens capsules were used by several research groups [24–26]. HCECs were cultivated on these biological substrates. Even though these substrates show good biocompability, they requires also donor tissues. So, in studies several natural coatings materials such as collagen type I, collagen type IV, fibronectin, laminin, gelatin, and albumin were tested to evaluate behavior of HCECs [27]. A study which conducted by Choi et al. shows that ECM protein coatings affect the HCECs' adhesion, proliferation, phenotype and function [28].

Natural and synthetic polymer based constructs were also developed by several groups to obtain corneal endothelial cell sheets. Watanebe et al. prepared hydrogel carrier by using gelatin [29]. Plastic compressed collagen gels which became collagen membrane like structure were also developed as a cell carrier for corneal endothelial cells transplantation [30]. Liang et al. (2011) produced a scaffold with blend of hydroxyethyl chitosan, gelatin and chondroitin sulfate [31], Ozcelik et al. (2013) developed ultrathin hydrogel films by using chitosan and poly (ethylene glycol) [32], in another study thermo-responsive cell culture carrier is acquired with the blend of poly(vinyl methyl ether) (PVME) and copolymer of vinyl methyl ether and maleic acid (PVMEMA) [22]. Poly (lactic acid) (PLLA) and poly (lactic-co-glycolic acid) (PLGA) were used as a biodegradable cell substrate for rabbit corneal endothelial cells [33]. Temperature-responsive polymer poly (N-isopropylacrylamide) (PIPAAm) is utilized for corneal endothelial cell sheet transplantation because of the ability of change its hydrophobicity/hydrophilicity according to temperature. Cells attach and proliferate on hydrophobic PIPAAm-grafted surfaces at 37 °C . Temperature is decreased to 20 °C, after incubation cells detach from the substrate. Lai et al. (2007) transplanted this obtained cell monolayer to rabbit corneas which stripped of endothelium via carrier gelatin hydrogel discs [34]. All these approaches are promising in terms of providing effective CE cell sheet.

2.4 Bioinspired Approaches to Corneal Recovery

Materials found in nature present superior properties that may be due to chemical properties unmatched by man-made materials or unique structures that manifest on different miniaturization scales. After hundreds of millions of years selection, these materials present unique solutions to human problems that may be seized by scientists in elaborate ways which are called bioinspired approaches [35]. From a tissue engineering point of view, the most relevant biological material is extracellular matrix (ECM) which provides chemical and structural support to cells. ECM is composed of different types of collagens, proteoglycans, glycosaminoglycans, laminins, glycoproteins, elastin and fibronectin. These components bind each other to form a stable substrate for cell growth, migration and differentiation while also binding adhesion receptors of cells. These adhesion receptors also carry signals from ECM into the cells to regulate a diverse range of processes such as differentiation, migration, survival and general homeostasis of the cell [36]. ECM also provides cell guidance by presenting a complex topography composed of pores, fibers and ridges on different scales. Often a primary topography found on the nanoscale formed by protein assemblies gives way to a secondary topography on the microscale created by bends or folds [37]. Cells respond to these topographical cues by changing their morphology and aligning themselves with topographical features in a process called contact guidance. Cell response depends on size and geometry of the features as well as physical and chemical properties of the substrate [38–40]. Cell response to mechanical properties of ECM also becomes relevant in a tissue engineering context since cells sense stiffness of their environment and respond accordingly. For example in vitro substrates that mimic ECM stiffness of bone tissue (34 kPa) induce osteoblast differentiation in mesenchymal stem cells (MSCs) while softer substrates with the characteristic stiffness of muscle tissue (11 kPa) direct these cells to muscle differentiation [41].

Measurements taken from different layers of human cornea with atomic force microscopy (AFM) show that each layer has different mechanical properties and elastic modulus values varying form 7,5 kPa to 110 kPa [11]. Descemet membrane layer which is in direct contact with corneal endothelium cells show an elastic modulus value of

50±17,8 kPa [10,11]. Studies show that corneal epithelial and endothelial cells respond to in vitro substrate stiffness. Epithelial cells show increased apoptosis and cytoskeletal disruptions on compliant substrates compared to stiffer ones [42]. Moreover corneal endothelial cells grow high density monolayers with cell geometries resembling that of in vivo tissue when substrate stiffness is matched with Descemets membrane while cells on tissue culture plates lose these properties [7]. Micro and nanotopography of cell substrates combined with ECM mimicking coatings were also shown to be effective at modulating corneal endothelial cell morphology viability and formation of tight junctions at cell interfaces [6]. Besides widely-used ECM components such as fibronectin, collagen, laminin and chondroitin sulfate [6], hyaluronic acid (HA) is also an important ECM component relevant in ophthalmology. Present in vitreous body of the eye, negatively charged long disaccharide chains of HA efficiently absorbs and retains water resulting in a lubricating effect [43] and high biocompatibility [44]. Because of these characteristics HA is utilized for corneal endothelial cell sheet engineering studies [45]. A large scale study conducted by Palchesko et. al. (2015) shows that mimicking Descemet's membrane ECM proteins and stiffness at the same time provide CECs better environment to maintain their normal phenotype throughout long term culture. Cell substrates whose elastic modulus is 50 kPa and coated with Col IV shows the best results among thirty-six different substrates [7].

2.5 Polyacrylamide Hydrogel as a Substrate

Polyacrylamide (PAAm) is a synthetic polymer composed of acrylamide monomers. PAAm hydrogels are acquired by free radical polymerization of acrylamide and crosslinker N, N'-methylenebis (acry1amide) monomers [46].

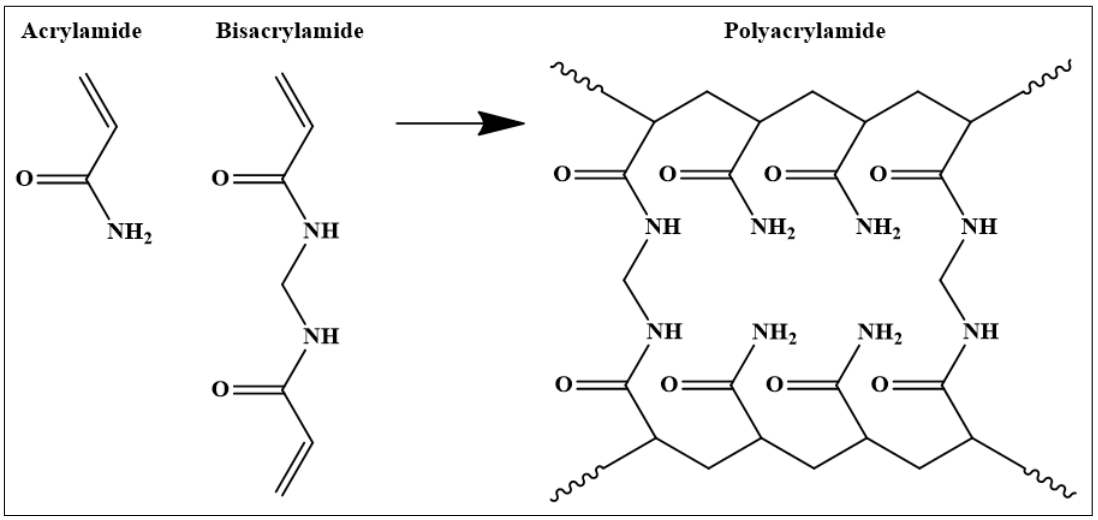

Figure 2.3 Free radical polymerization of acrylamide.

Polyacrylamide hydrogels (PAAm) has been preferred for lots of studies because of their remarkable properties. PAAm hydrogels widely used for mechanobiology studies [47–49], since the stiffness values of PAAm hydrogels can be simply regulated by changing crosslinker amount without altering chemical characteristics. PAAm hydrogels have chemically and biologically inert surface but extracellular matrix proteins can be attached to the surface of the hydrogels covalently in order to enhance surface bioactivity. Moreover, PAAm gel has an excellent optical quality and its porous structure is more suitable as a physiological environment than other surfaces [50]. Briefly, its inertness, transparency and flexibility makes polyacrylamide suitable material for our research purposes.

3. MATERIALS AND METHOD

3.1 Surface Preparation

3.1.1 Preparation of Flat Polyacrylamide Substrates

Polyacrylamide hydrogels were used as a substrate to mimic corneal endothelium micro-environment. Flat polyacrylamide hydrogels were prepared between plastic petri dish surface and activated coverslips. To activate coverslips, round coverslips (14 mm) were placed into falcon tube (50ml) and cleaned with 0.1 M NaOH solution. After they were rinsed thoroughly, they were kept in ethanol for half an hour on mixing rotator. Then coverslips were immersed in 2% 3-aminopropyltrimethoxysilane (APTES) solution (in ethanol) for half an hour on mixing rotator. After they were rinsed several exchange of deionized water (DI) with stirring for ten minutes in each. Later, coverslips were immersed in 1% glutaraldehyde solution (in DI) for half an hour on stir plate. Coverslips were again washed by several exchanges of DI with stirring. Finally they were dried at room temperature by avoiding coverslips get dusty. When they will be used for cell culture, they were transferred in 70% ethanol and dried in the laminar flow hood [48, 51].

After activation of coverslips, polyacrylamide hydrogels were prepared between these activated coverslips and plastic petri dish surfaces. To make ready pre-polymer solution, stock solutions were prepared. 40% w/v acrylamide (AAm) solution in phosphate buffer saline (PBS), 2% w/v N,N'-Methylenebisacrylamide (Bisacrylamide) solution in distilled water were made ready. Tetramethylethylenediamine (TEMED) solution was formed by diluting 1:10 in distilled H2O. 200 mM Ammonium persulfate (APS) solution was prepared in distilled water. These chemicals were purchased from Sigma-Aldrich. Working solution consisting of 15% (w/v) acrylamide monomer and 0.3% (w/v) bisacrylamide cross-linker was prepared. This working solution was vortexed and degassed for 15 minutes. As an accelerator TEMED, then as a free

radical initiator APS solution was added to the degassed pre-polymer solution for gel polymerization [47, 52, 53].

50 μl of this solution was dropped onto the glass slide and activated coverslip was placed on the top of droplet. After gel solution coat the entire surface of coverslip, resulting of polymerization was waited. Amount of gel solution which dropped was adapted from Aratyn-Schaus Y., et al. (2010). After completion of polymerization, coverslip which attached with the polymerized hydrogel was segregated from the glass slide. Coverslip attached hydrogels were kept in ddH2O to provide hydration [48].

Round glass coverslips with 14 mm diameter were used to prepare flat and patterned PAAm hydrogels at the beginning of the study, but activation of coverslips was very time consuming and did not allow preparation great number of samples at the same time. If the coverslip surfaces do not properly washed between procedure's steps or do not completely activate for any reason, gels shrink on coverslips after polymerization. Therefore, GelBond® PAG films were used for study. GelBond® PAG film is commercial product which formed by polyester and produced for polyacrylamide hydrogels. These transparent films were also used in literature [52]. GelBond films were cut into rounds with a diameter of 14 mm. Before hydrogel synthesis, both side of films were exposed to UV light for 15 minutes in each for sterilization. After sterilization, PAAm hydrogels were synthesized by the method used in coverslips.

3.1.2 Preparation of Bio-Inspired Polyacrylamide Substrates

In bioinspired approach, hexagonal structure of healthy human corneal endothelial cells was formed onto Silicon wafer by using photolithography technique and this structure was transferred to polyacrylamide surfaces via soft lithography technique. For this purpose, firstly silicon wafer molds was designed and prepared according to following procedure. Si wafer molds were produced at Bilkent University National Nanotechnology Center with Assist. Prof. Dr. Çağlar Elbüken's consultancy.

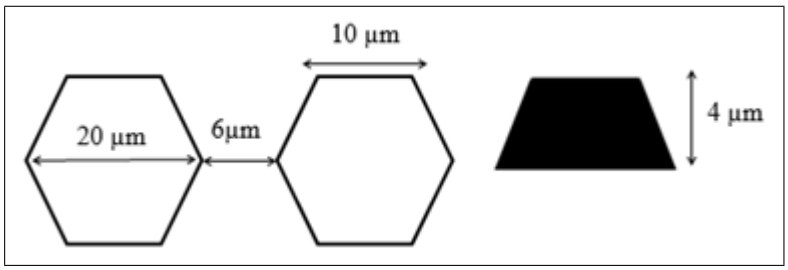

Figure 3.1 The shape, the depth and dimensions of the hexagonal pattern on the Silicon wafer and the distance between patterns are prepared by inspired from healthy corneal endothelium [2, 3].

In order to fabricate hexagonally shaped patterned mold, MicroChem SU-8 2005 negative photoresist and Si wafer were used. Since UV applied, negative photoresist turns into insoluble in developer solution, hexagonal patterns on Si wafer were obtained.

1. **Cleaning the substrate (Si wafer):** Si wafer which creates pattern was cleaned with acetone, isopropyl alcohol and deionized water. After drying with nitrogen gas, it was held at 120 °C for a few minutes for dehydration. Then it was cooled to room temperature.

2. **Coating the first adhesive layer using SU-8 2005:** Firstly, Si wafer was coated with MicroChem SU-8 2005 uniformly by using spinner (Spinner, Laurell, WS650SZ-6NPP-lite), which is present in the Bilkent University UNAM clean room. The required spinner parameters for first layer was entered. Following step is soft baking. The wafer was put on 65 °C hot plate and waited for 2 min. After 2 min, it was put on 95 °C hot plate for 4 min. Finally, it was put on 65 °C for 1 min. Then the wafer was cooled to room temperature. Baking process provides that the photoresist is ready for exposure. The next step was exposing the photoresist and achieving cross linking. EVG 620 mask aligner and the required settings for this exposure system were used. After exposure, it is needed to bake the wafer. This process is named as post-exposure baking (PEB). Post exposure bake includes three step process. First the wafer was put at 65 °C for 1 min, then at 95 °C for 3 min, finally the wafer was baked at 65 °C for 1 min. After PEB, the wafer was cooled down to room temperature.

3. **Coating the second SU-8 2005 layer and patterning:** At this step, very similar processes to the first layer were applied. There was a small difference that the thickness of this layer should have been controlled in order to control the height of the features. Required spinning settings to obtain a 4 um height coating were used. After steps of soft baking, exposing the photoresist through the mask and achieving cross linking, post-exposure baking was applied as in the first step.

4. **Development:** Lastly, MicroChem SU-8 Developer solution was prepared in a glass beaker and the Si wafer was immersed in this solution for 6 min to remove the unexposed parts of the wafer. In that time beaker was mixed in a circular motion. Then wafer was cleaned with nitrogen gas. The features are built on the top of the silicon wafer was observed by using upright microscope.

Procedure is organized according to devices which placed in Bilkent University UNAM's clean room.

Soft lithography technique was used to transfer the patterning on the Silicon wafer to the PAAm substrates. Pre-polymer solution which includes AAm, Bisacrylamide and distilled water were added into eppendorf tube. After adding TEMED and APS solution, 50 μl of pre-polymer solution was dropped onto the one pattern of silicon wafer, then sterilized GelBond® PAG film was placed on the top of this droplet. Gel solution covers the whole hydrophilic surface of film and gel polymerization was waited. After about two hours gel attached films were carefully removed from the silicon wafer mold with the help of tweezers. Before remove the coverslips, to make easier separation of gel from the mold, distilled water was added onto the polymerized gels. After all, hexagonally shaped patterned polyacrylamide hydrogels were obtained.

3.1.3 Chemical Modification of Polyacrylamide Substrates

3.1.3.1 Modification of Polyacrylamide Substrates via Sulfosucci- nimidyl 6 (40- azido -20-nitrophenylamino) Hexanoate (Sulfo-SANPAH)

20 mg Sulfo-SANPAH powder was dissolved in 400 μl DMSO, then immediately 40 μl working aliquots were prepare and stored at $-80\,^{\circ}$C for later uses. One of 40 μl working aliquots was diluted in 10 ml distilled water. 300 μl of this Sulfo-SANPAH solution (0,2 mg/ml) was poured onto each polyacrylamide hydrogel and gel surfaces were exposed to UV light (at around 5 cm distance) for about 30 minutes. After Sulfo-SANPAH's color had changed from red to brown, gels were washed several times with deionized water. 1 mg/ml Col IV solution (in 0.1 M acetic acid) and 1mg/ml hyaluronic acid solution (in deionized water) was prepared and pipetted onto gel surfaces with different amounts then they were kept waiting for overnight at $4\,^{\circ}$C. Table 3.1 shows coating materials amount poured on hydrogels. Next day gels were washed with several washes of distilled water and incubated in cell growth medium for two hours. After this step, coated hydrogels were ready for cell studies [48]. Figure 3.2 represents modification of PAAm hydrogels via Sulfo-SANPAH.

Table 3.1
Chemical Modification Groups.

Experimental Groups	Coating Amounts
Plain	-
Col IV coated	30 μl Col IV solution + 270 distilled water
HA coated	30 μl HA solution + 270 distilled water
50%-50% Col IV-HA	15 μl Col IV + 15 μl HA solution + 270 distilled water
75%-25% Col IV-HA	22,5 Col IV + 7,5 μl HA solution + 270 distilled water
25%-75% Col IV-HA	7,5 Col IV + 22,5 μl HA solution + 270 distilled water

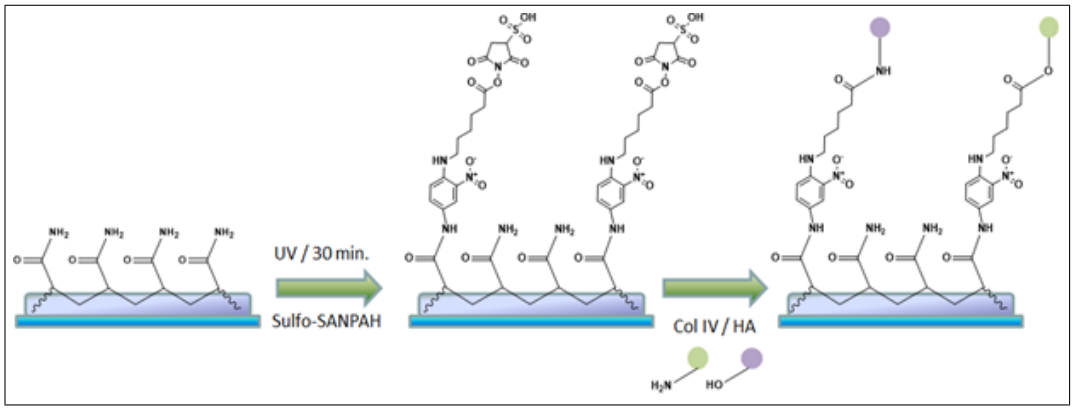

Figure 3.2 The schematic representation of PAAm hydrogel modification via Sulfo-SANPAH.

3.2 Characterization of Substrates

3.2.1 Characterization of Mechanical Properties of PAAm Hydrogels

Hydrogel materials is widely used in tissue engineering applications and their mechanical properties are the key elements for especially mechanobiology studies. Several mechanical testing techniques are used for hydrogel materials such as tension test, compression test, confined compression test, indentation, shear rheometry, dynamic mechanical analysis and atomic force microscopes (AFM) indentation [54]. Rheology analysis and tension test were applied for our hydrogel samples.

3.2.1.1 Rheology Analysis

Polyacrylamide hydrogels which have different elastic modulus were prepared by using two different recipes from literature. Working solution of sample A contains 15% AAm and 0.3% Bisacrylamide, while B contains 10% AAm and 0.03% Bisacrylamide [51, 52].

Three samples of each were prepared and kept in DIH_2O when they reach to swelling equilibrium. After they reached the equilibrium degree of swelling, rheometer analysis was performed. Elastic modulus of PAAm hydrogels were measured using a rheometer at Yıldız Technical University Central Laboratory (Malvern Bohlin range, CVOR 150). Experiment was performed at 0.01 strain and between 0.01 Hz-100.00 Hz frequencies [55].

3.2.1.2 Tension Test

Elastic modulus of stiffer gels was also determined by tensile testing. Hydrogel samples were gripped attentively between flanges of the instrument. The rate at which experiment were performed is 100mm/min. Samples have dimensions approximately 5 mm in thickness, 9 mm in width and gauge length was 35 mm. Lloyd LF Plus instrument was used for experiment (n=8).

3.2.2 Characterization of Morphological Properties Polyacrylamide Hydrogels

Patterned polyacrylamide substrates were characterized by using optical microscopy. After peeling away from silicon wafer mold, surfaces of the hydrogels were dried with N2 and optical images were taken with the help of optical microscopy (Leica, DTC295).

3.2.3 Characterization of Chemical Properties Polyacrylamide Hydrogels

3.2.3.1 Fourier Transform Infrared Spectroscopy (FTIR) Analysis

The chemical content analysis of substrates resulted from modifications was investigated via Fourier Transform Infrared Spectroscopy. FTIR spectra was recorded

the range of 4000 to 500 cm^{-1}. Plain PAAm hydrogel, uncoated only Sulfo-SANPAH treated PAAm hydrogel, only Col IV coated, only HA coated, and 50%-50% Col IV/HA coated PAAm hydrogels were examined. The FTIR measurements were perfomed at Hacettepe University Advanced Technologies Application and Research Center using Attenuated Total Reflectance Fourier Transform (ATR- FTIR) spectrophotometer.

3.2.3.2 Water Contact Angle Measurements (WCA)

Water contact angle measurements were performed by using unmodified and modified hydrogels (n=4). All measurements were done by dropping a water droplet of purified water of approximately 3 μl volume on the surface of each hydrogel followed by 15 second long imaging with 1 second intervals [56]. Contact Angle Measurement Instrument (CAM 100, KSV) was used at Bogazici University, Department of Chemistry was used.

3.2.3.3 Swelling Ratio

Hydrogel samples were prepared and swelling test was done to determine swelling ratio at the equilibrium. The samples were weighted after polymerization, and then samples were placed in 6-well plate. Swelling tests were done with Dulbecco's Modified Eagle Medium (DMEM)-High Glucose, Capricorn which have used for cell culture studies. Hydrogels with 14 mm diameter immersed in DMEM containing 6-well plate. The weight of swollen samples was measured at determined time intervals. Measurements was taken at 5 min, 10 min, 30min, 60min, 24 h, 48 h, and 72 h. Before the samples were weighted, excess water was removed from the samples and measurement was done at room temperature.

The swelling ratio was determined from the following equation,

$$S(\%) = \frac{m_t - m_0}{m_0} X100 \tag{3.1}$$

where m_t represents the weight of swollen hydrogel after time point t while m_0 is the initial weight of hydrogel after polymerization at time point zero [57].

3.2.3.4 Characterization of Chemical Modifications with Immunostaining

After hydrogel substrates modified with Col IV, HA and mixtures with their different amounts, immunostaining analysis was performed to demonstrate success of coating. Anti-Hyaluronic acid (ab53842) and Anti-Collagen IV (ab6586) primary antibodies, and Donkey Anti-Rabbit IgG H&L (Alexa Fluor® 555) preadsorbed (ab150062) and Donkey Anti-Sheep IgG H&L (Alexa Fluor® 488) (ab150177) secondary antibodies were used.

Blocking solution which contains 1% BSA and 22.52 mg/mL glycine was prepared in PBST (PBS+ 0.1% Tween 20). 300 μl blocking solution was added on hydrogels for 30 min to block unspecific binding of the antibodies. Primary antibodies were diluted 1/200 in 1% BSA in PBST. Secondary antibodies were diluted 1/300 in 1% BSA in PBST. 150 μl of primary antibody solution and 150 μl of secondary antibody solution were added onto each gel and incubated overnight at 4 °C. After aspiration of excess antibody, gels were washed with PBSt three times five minutes every wash. Then, 150 μl of each both secondary antibody solution was added to each gel and incubated for 1 hour at room temperature. After one hour excess solution was removed and gels were washed with PBS three times in dark [58].

Only secondary antibodies were added onto different samples in same experimental groups as a control group. Immunofluorescence images of unmodified and modified substrate were taken (Leica, DTC295).

3.3 Cell Culture Studies

3.3.1 Cell Viability and Proliferation

In order to investigate the behavior of CECs against stiffness, ECM coatings and bioinspired topography of polyacrylamide hydrogels, BCE C/D-1b (ATCC® CRL-2048™) cell line was used. BCE C/D-1b cells are bovine corneal endothelial cells. This cell line was obtained from adult bovine corneas. It is known that while their doubling time is around 55 hours at passage 70, this time decreases to 30 hours at passage 90 [59, 60]. The viability of cells on the prepared different substrates was measured with the tetrazolium dye 3-(4,5-dimethylthiazol-2-yl) -2,5- diphenyltetrazolium bromide (MTT) assay. Cell cultures studies were carried out on the prepared flat, modified flat, bioinspired and modified bioinspired PAAm surfaces. DMEM High Glucose (4.5 g/l), with L-Glutamine, with Sodium Pyruvate (Capricorn Scientific, DMEM HPA) was used as a culture medium. Complete medium contained also 10% v/v Fetal Bovine Serum (FBS) and 1% v/v antibiotic. The effect of coating materials and surface topography on cell viability was investigated. 20.000 cells were seeded each well of 24 well-plates and maintained at 37 °C, 5% CO_2. Viability of cells was measured on 1^{st}, 4^{th} and 7^{th} day of culture [61].

After culturing BCECs on hydrogels, MTT assay was performed on stated days. MTT solution was prepared in PBS with 5 mg/ml concentration. 40 μl MTT solution was added to each well. Plates were incubated for three and half hour. Before the measurement, MTT solution containing medium was removed and 250 μl Dimethyl Sulfoxide (DMSO) was added to each well. After mixing for a while on gentle shaker. 100 μl of each well's solution was taken and transferred to 96-well plate. Cell viability was determined by measuring the optical density of the formazan crystals dissolved DMSO solution at 570nm and 750nm as reference wavelengths using a Micro-plate Reader Spectrophotometer (BIO-RAD iMark, Microplate Reader). Table 3.2 shows experimental groups for cell culture studies. Table 3.3 shows the summary of experimental procedures.

Table 3.2
Experimental groups for Cell Studies

Flat	Patterned
Col IV coated	Col IV coated
HA coated	HA coated
50%-50% Col IV-HA	50%-50% Col IV-HA
75%-25% Col IV-HA	75%-25% Col IV-HA
25%-75% Col IV-HA	25%-75% Col IV-HA

3.3.2 F-actin Staining

Cells grown on flat and patterned PAAm substrates for 7 days were washed with warm PBS 3 times for 5 minutes. Cells were fixed with 3.7% formaldehyde for 10 minutes and then permeabilized with 1% tritonX-100 solution for 10 minutes. Non-specific binding of phallotoxin was blocked with 1% BSA solution for 30 minutes. 6.6 μM phalloidin-Alexa Fluor 488 conjugate methanolic stock solution was dilutied in PBS (1:40) and added onto cells. After incubating for 30 minutes, cells were washed with 1% BSA solution 3 times for 5 minutes. DAPI counter-staining was performed by incubating cells in DAPI staining solution (300 nM) for 3 minutes and washing with PBS. Images were taken with blue and violet excitation filters for Alexa Fluor 488 and DAPI, respectively [7].

3.3.3 Statistical Analysis

ANOVA method was used for statistical analysis of MTT results. With the value of $p<0.05$, Tukey's multiple comparison test was used to determine the difference between experimental groups. The data were demonstrated to be as means $\pm$ standard error.

Table 3.3
Summary of experimental procedures.

Step	Experimental Procedure
1	Preparation of Flat PAAm Hydrogels
2	Preparation and Characterization of Bioinspired PAAm Hydrogels
3	Modification of Substrates with Col IV and HA
4	Characterization of Modified PAAm Structures
5	Cell Culture Studies of Prepared Corneal Endothelial-like Structures

4. RESULTS

Flat and bioinspired PAAm hydrogels were prepared and modified with Col IV and HA. Mechanical, morphological and chemical characterizations was performed to be able to characterize unmodified and modified PAAm substrates. After characterization, cell culture studies were performed on these prepared cell substrates. Results of characterizations and cell culture studies were presented in this chapter.

4.1 Mechanical Characterization Results

Gels synthesized according to two different recipes with different cross-linker concentrations (0.3 % and 0.03 %) were first characterized with rheometer. The resulting values of storage modulus (G'), loss modulus (G") and delta (δ) were represented in graphs as shown in the example in Figure 4.1. Horizontal axis represents each frequency covered during the frequency scan. The results for softer hydrogels with a cross-linker concentration of 0.03% show that G' values are much larger than G" values consistently for all frequencies which indicates that samples show close-to-ideal elastic properties. G'/G" ratio which equal tan δ values also show that these values are below 1 indicating elastic gel behavior [55].

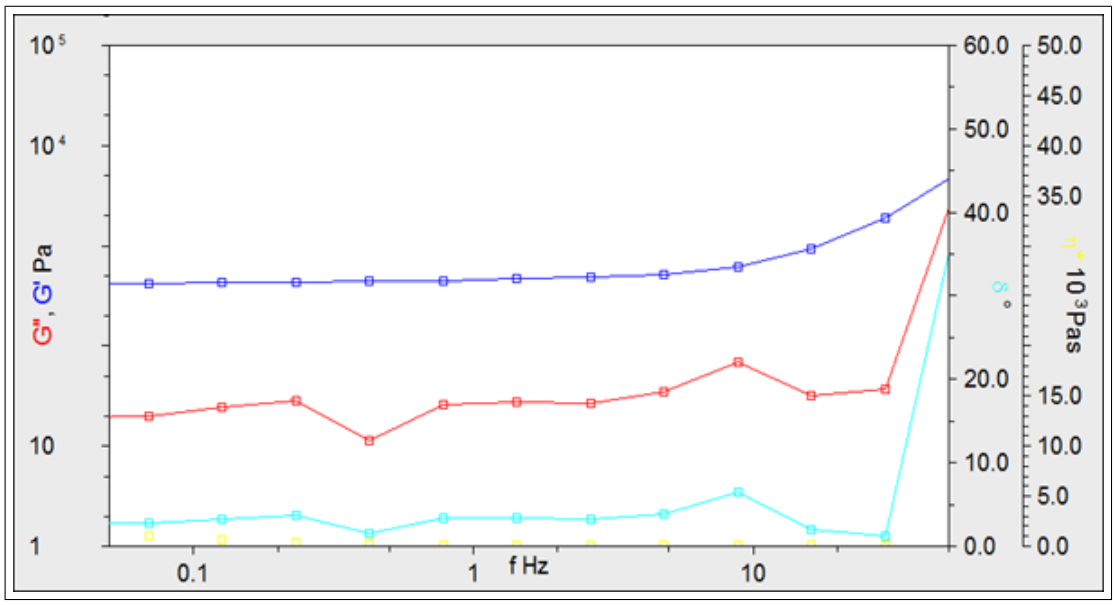

Figure 4.1 Rheometer frequency scanning of a polyacylamide gel with 0.03% cross-linker ratio.

Rheometer results for soft hydrogels show consistent results up to 10 Hz and values around 1 Hz were used previously in the literature for gels with our expected stiffness values. Machine generated results at the frequency of 1.438 Hz were given at Table 4.1.

Table 4.1
Rheometer measurements at 1.438 Hz for gels with 0.03% cross-linker ratio.

Strain	Elastic Modulus (Pa)	Viscous Modulus (Pa)	Complex Viscosity (Pa)	Shear Stress (Pa)	Tan Delta
0.009976	322.80	20.88	38.41	2.942	0.06469
0.009885	459.70	21.93	50.92	4.275	0.04772
0.009862	462.50	27.39	51.27	4.296	0.05922

Elastic moduli calculated by device give an average value of 0.42 ± 0.080 kPa. Stiffer gels with a cross-linker concentration of 0.3%, which are to be used in cell

culture experiments, did not show the same consistency in the covered frequency range as rheometer devices become unreliable for higher elastic moduli. For these gels, tensile testing was performed in order to determine elastic moduli. An example stress-strain curve for one of these samples was given in Figure 4.2. Elastic moduli generated from these curves by measuring the slope gives an average of 71.81 ± 9.78 kPa (n=8).

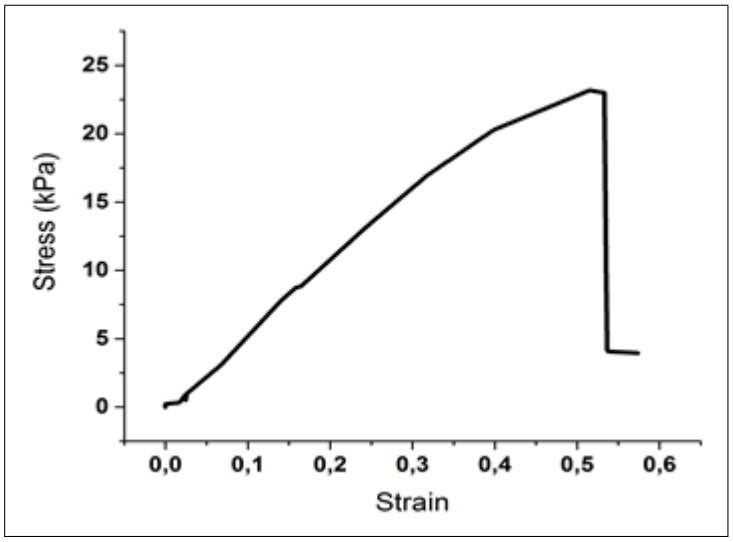

Figure 4.2 Stress-strain curve for stiff PAAm hydrogel.

4.2 Morphological Characterization Results

4.2.1 Optical Microscopy

Optical microscopy images of flat PAAm hydrogels and PAAm hydrogels bioinspired from healthy corneal endothelium were shown in Figure 4.3. Flat gels show no features on the surface while hexagonal troughs are clearly visible on patterned gels.

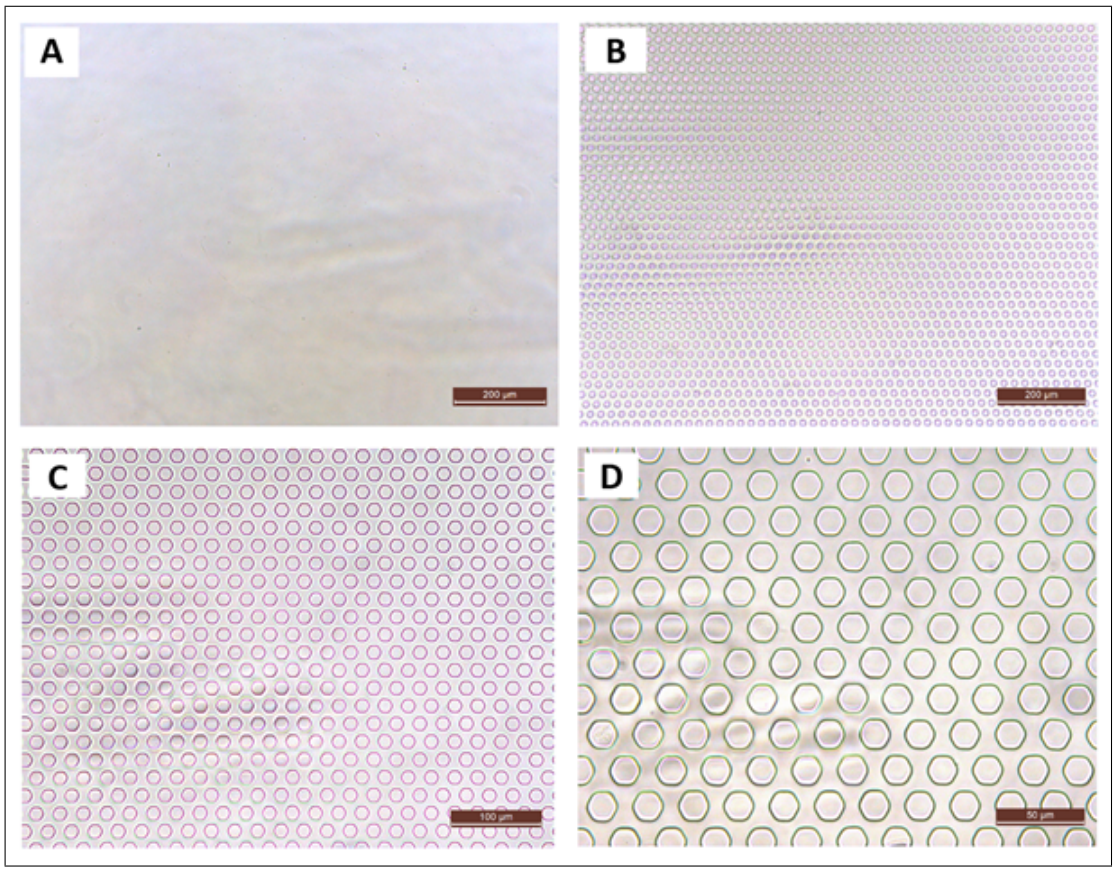

Figure 4.3 Optical microscopy image of A) Flat PAAm hydrogel, B) Bioinspired PAAm hydrogel at 10x Magnification, C) Bioinspired PAAm hydrogel at 20x Magnification, D) Bioinspired PAAm hydrogel at 40x Magnification.

4.3 Chemical Characterization Results

4.3.1 Fourier Transform Infrared Spectroscopy (FTIR) Analysis

First of all FTIR spectrum of a plain hydrogel was obtained in order to confirm chemical purity and stability of our reagents. Figure 4.4 shows the spectrum where sharp peaks are visible at wavenumbers 1413 cm^{-1}, 1449 cm^{-1}, 1612 cm^{-1}, 1651 cm^{-1} and 3191 cm^{-1}.

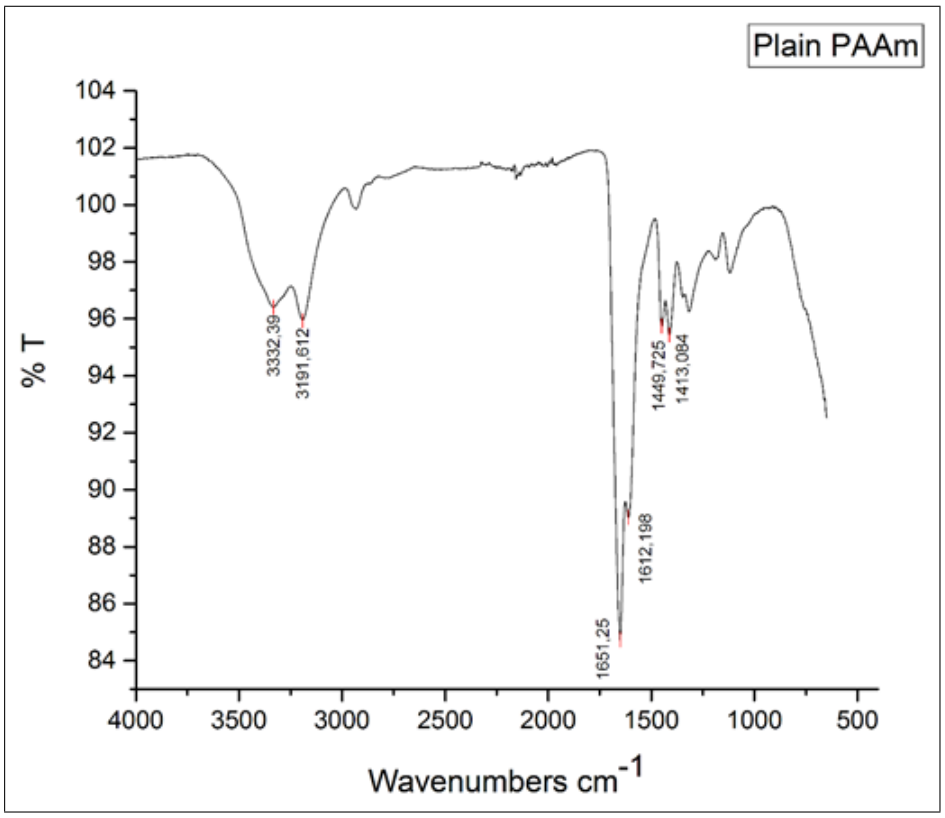

Figure 4.4 FTIR spectrum of unmodified PAAm hydrogel.

After modification of PAAm gel surfaces with Col IV and HA using sulfo-SANPAH method, FTIR spectra were obtained from each gel. Overlaid spectra of gels modified with Col IV, HA and a mixture thereof were shown in Figure 4.5 along with the spectrum of unmodified PAAm hydrogel. All of these spectra were identical in the overlaid graph.

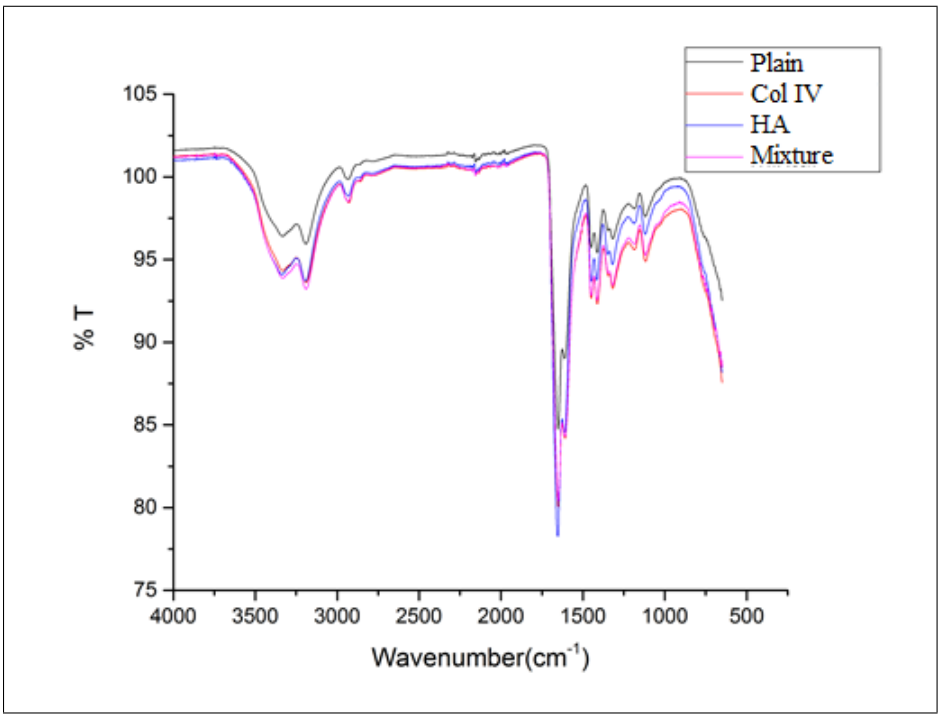

Figure 4.5 FTIR spectra of unmodified and modified PAAm hydrogels.

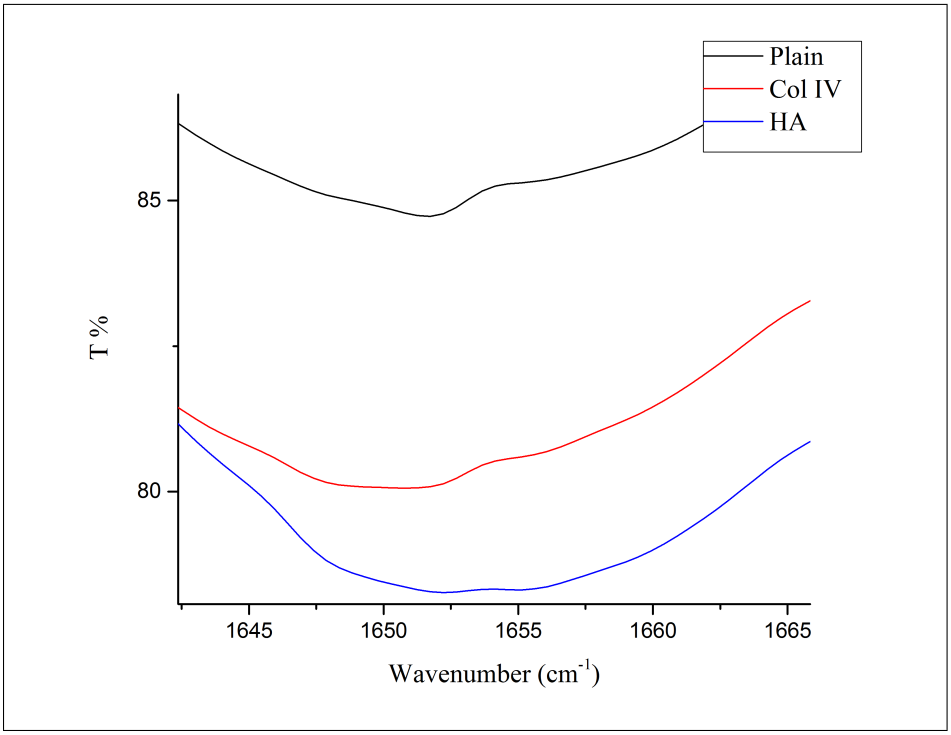

Figure 4.6 FTIR spectra of unmodified and modified hydrogels zoomed between the wavenumbers 1640 and 1665 cm^{-1}.

The lack of any differences between plain and coated hydrogel spectra required a search for subtle differences which can be seen in Figure 4.6 where Col IV coated hydrogel has slightly lower transmittance at 1650 cm^{-1} and HA coted hydrogel changes the spectrum shape due to an increased absorbance at 1655 cm^{-1}.

4.3.2 Water Contact Angle Measurements

Contact angles of unmodified PAAm and modified PAAm were measured by using CAM 100, USA and shown in the Table 4.2. Contact angles were calculated as 33.1 ± 3.2°, 110.3 ± 4.3°, 65.2 ± 4.4°, 95.4 ± 2.1° for plain, col IV coated, HA coated and 50/50 Col IV/HA coated PAAm hydrogels, respectively. Figure 4.7 shows the images of the water contact angle of PAAm hydrogels.

Table 4.2
Water Contact Angle of PAAM Hydrogels (n=4).

Experimental Group (PAAm)	Water Contact Angle
Plain	33.1 ± 3.2°
Col IV coated	110.3 ± 4.3°
HA coated	65.2 ± 4.4°
Mixture coated	95.4 ± 2.1°

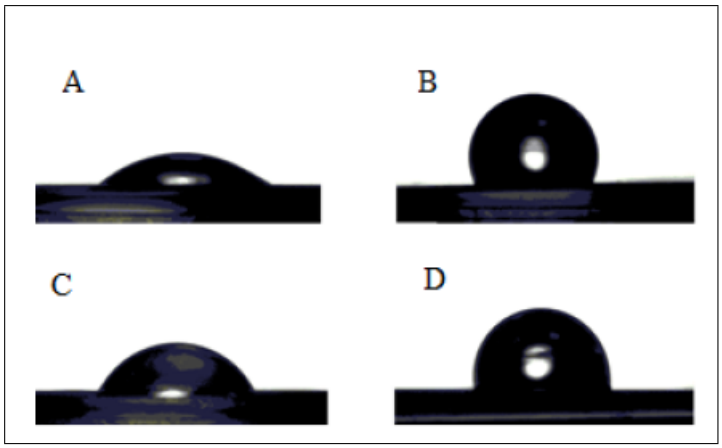

Figure 4.7 Water Contact Angle of PAAm Hydrogels (n=4). A) Plain PAAm, B) Col IV coated PAAm, C) HA coated PAAm, D) Mixture coated PAAm.

4.3.3 Swelling Ratio

Swelling test was performed to determine time to reach to the equilibrium of swelling. Figure 4.8 shows that swelling % of stiff PAAm hydrogel (15% AAm and 0.3% Bisacrylamide) as function of time. As shown in graph the weight of swollen hydrogel is almost fixed after 48 hours and hydrogels reach to equilibrium of swelling after this time. Swelling Ratio was determined as 59.96 ± 3.93.

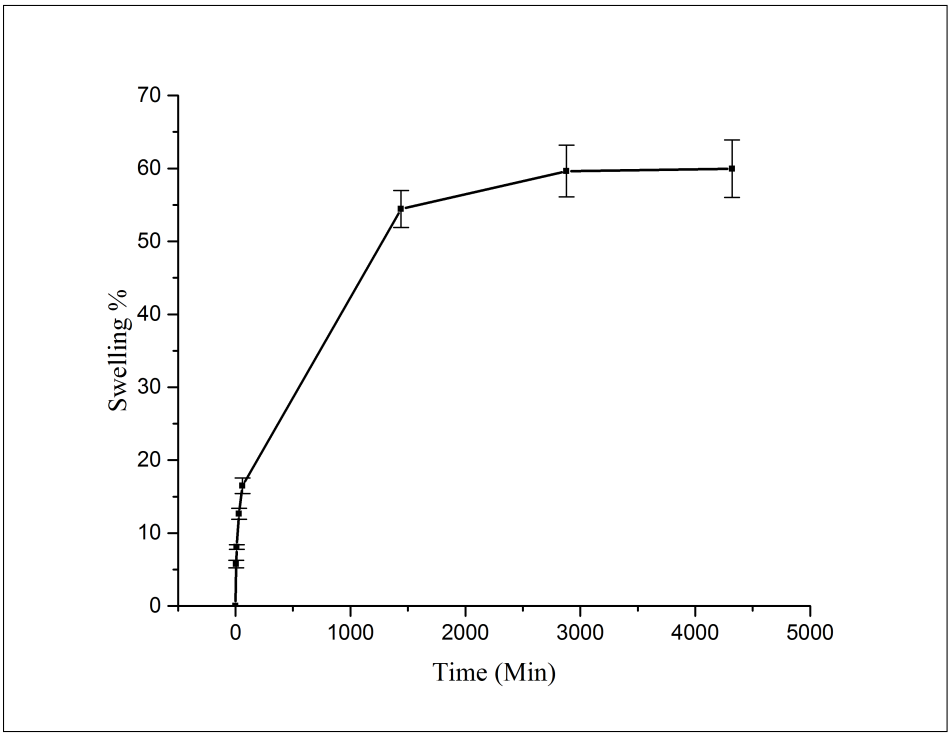

Figure 4.8 Swelling [%] as function of time for stiff PAAm hydrogel in DMEM at RT.

4.3.4 Immunostaining Results

Fluorescence microscope images obtained after staining covalently bound Col IV and HA with corresponding primary and secondary antibodies were shown in Figure 4.9. Alexa Fluor 488 conjugated secondary antibody labels HA and gives green fluorescence while Alexa Fluor 555 conjugated secondary antibody selectively labels Col IV bound primary antibodies to give a red fluorescent signal. Background images which are taken from substrates treated only with secondary antibodies show significantly

lower fluorescence signals in all groups. In the case of equal mixture of Col IV and HA, Col IV signal is much stronger than HA signal. Fluorescence microscope images were taken with corresponding excitation filter of each secondary antibody. Excitation of a sample with the filter corresponding to the coating material absent from the sample gave no signal at all. For example exciting Col IV coated samples with blue filter gives no signal.

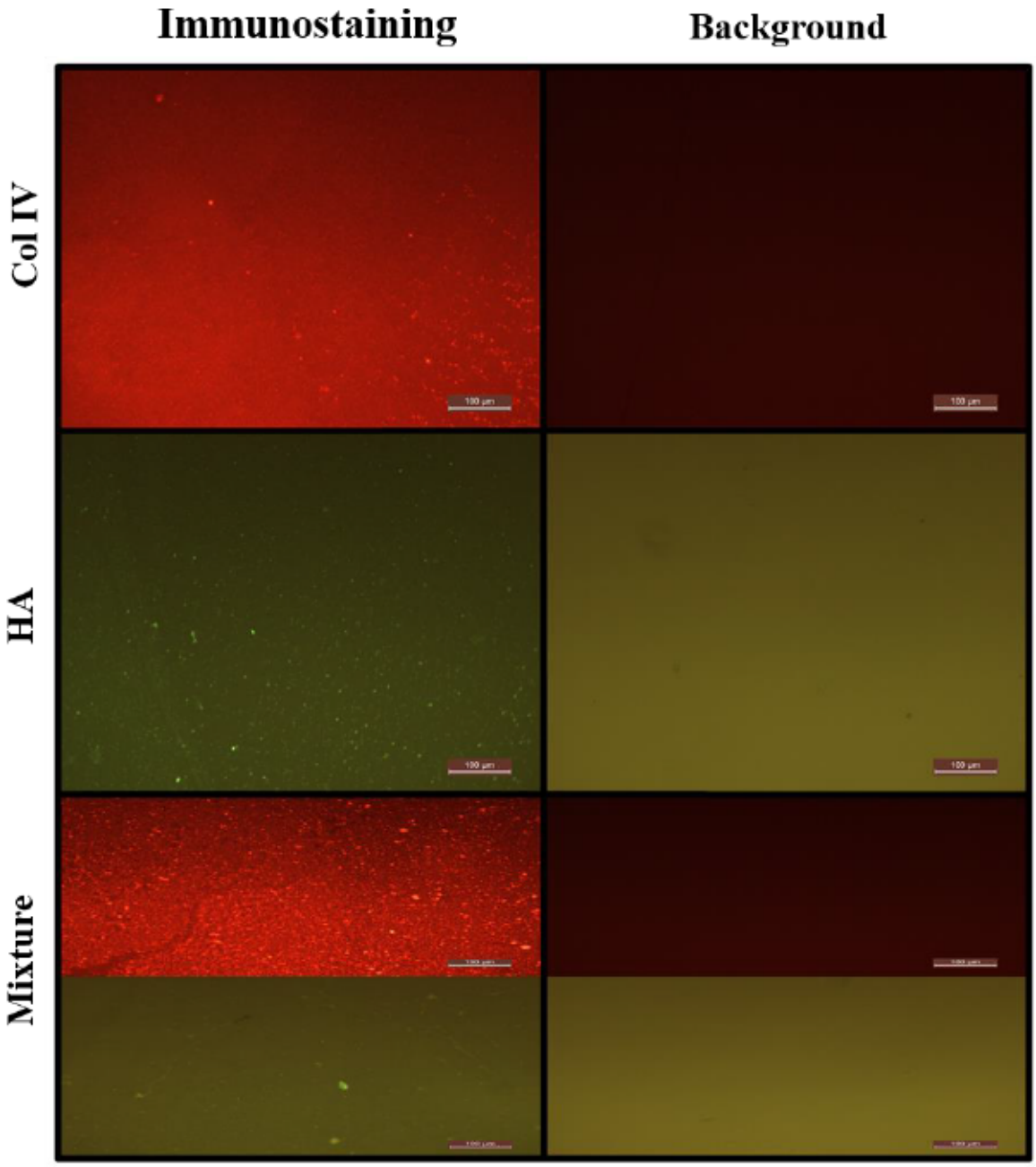

Figure 4.9 Immunostaining and background images of modified hydrogels.

4.4 Cell Culture Studies

4.4.1 Cell Viability and Proliferation

The effect of surface topography and chemical composition were investigated by using MTT assay. CECs were seeded and cultured on flat and patterned hydrogels with different coating compositions and tissue culture polystyrene (TCP) plates. In order to determine cell viability and proliferation on prepared substrates, MTT assay was used for 1^{st}, 4^{th} and 7^{th} days of incubation (n=4). Figure 4.10 shows Bovine Corneal Endothelial Cells (BCE C/D-1b) on TCP under optical microscopy.

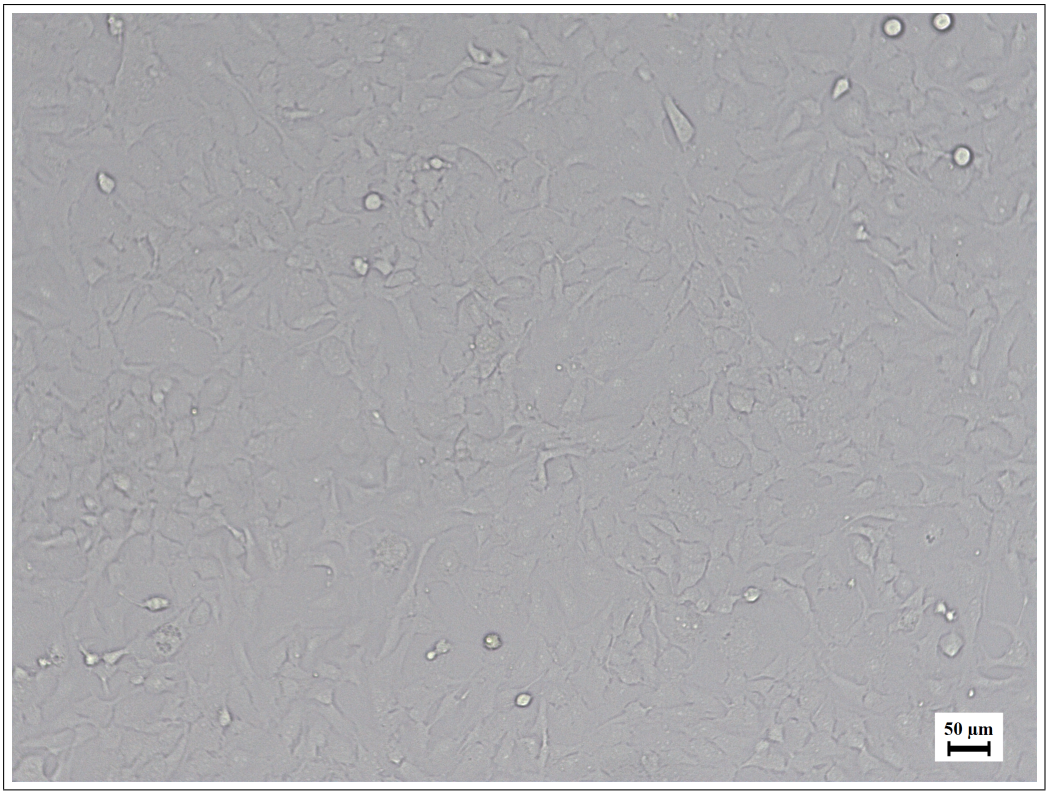

Figure 4.10 Optical Microscopy image of Bovine Corneal Endothelial Cells (BCE C/D-1b) on TCP.

The results of MTT assay at 1^{st} day was shown in Figure 4.11. According to results, it was observed that patterned Col IV coated substrates significantly different from flat Col IV coated substrate. The same positive effect of cornea endothelium bioinspired surface topography appears in HA coated hydrogels as well.

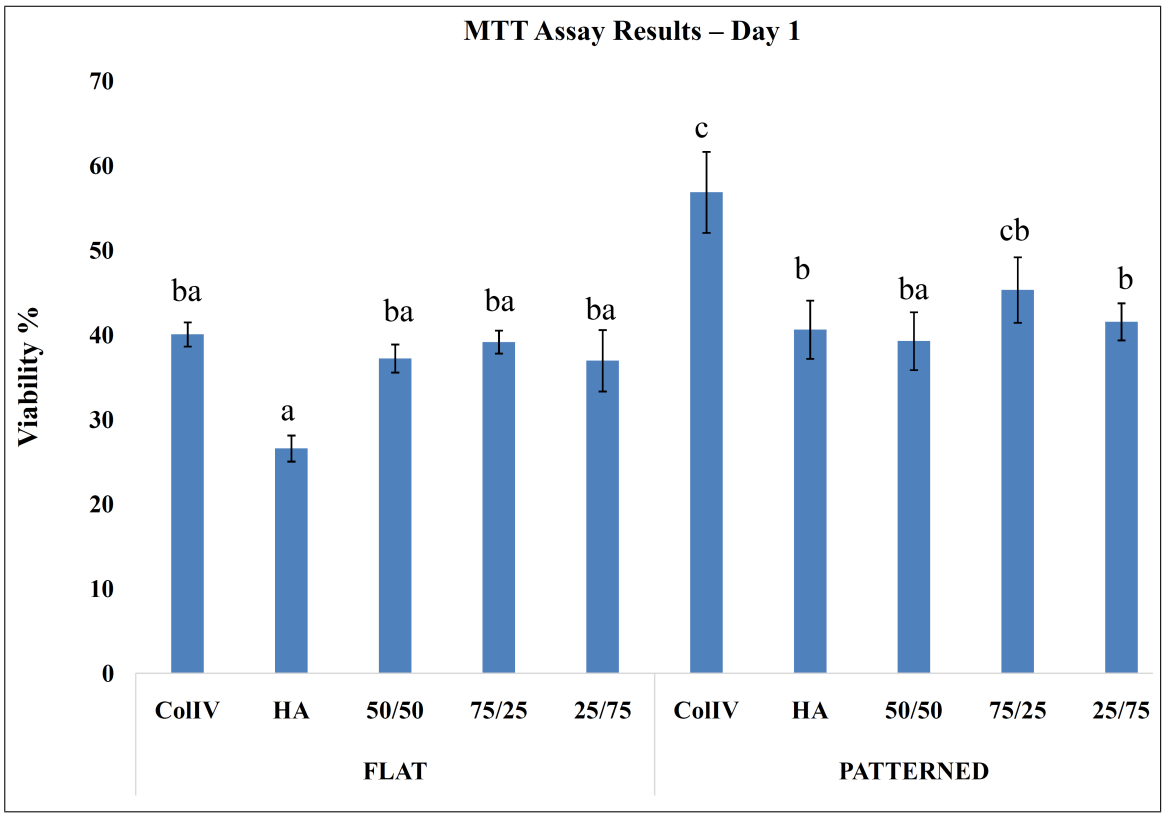

Figure 4.11 MTT assay results at 1^{st} day. Data is expressed in means ± SE ($p < 0{,}05$).

The results of MTT assay at 4^{th} day was shown in Figure 4.12. At day 4, similar to day 1, viability ratio in patterned hydrogels exceeded that of flat with the exception of 50/50 Col IV/HA ratio coated hydrogels.

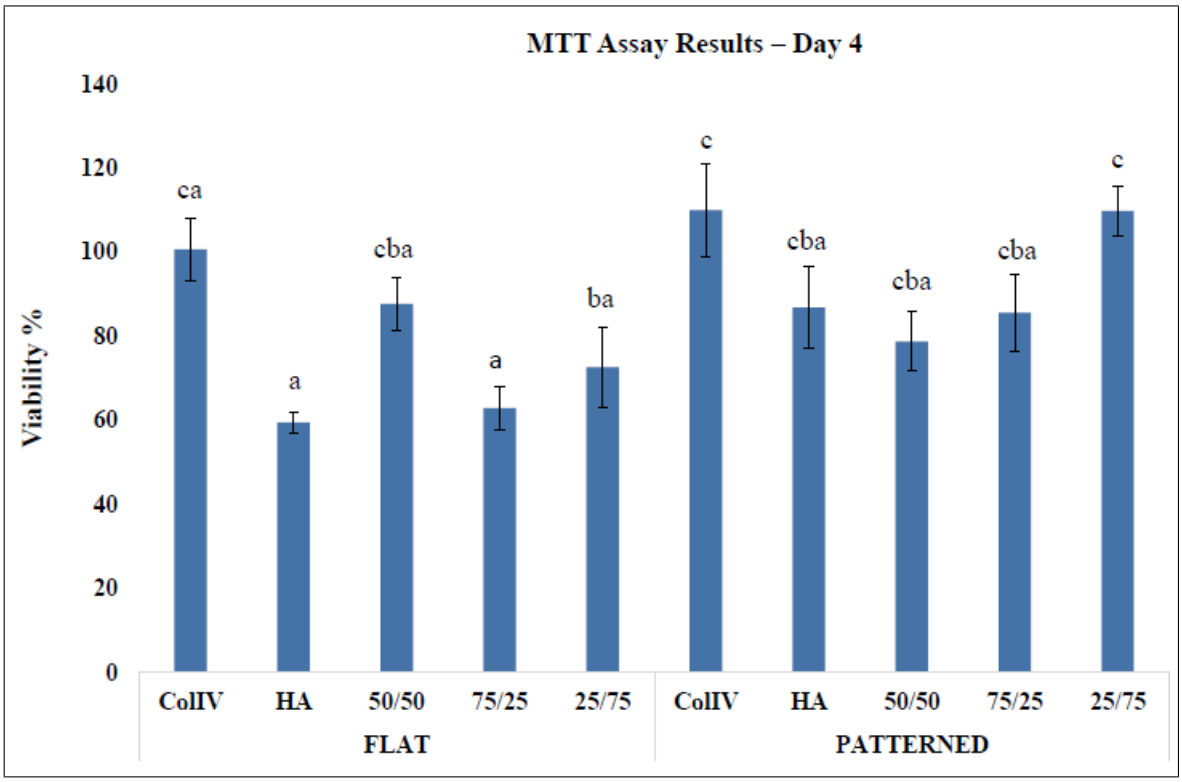

Figure 4.12 MTT assay results at 4^{th} day. Data is expressed in means ± SE ($p < 0{,}05$).

MTT results at 7^{th} day was shown in Figure 4.13. Col IV and 25/75 Col IV/HA ratio coated substrates show highest cell viability on flat substrates on day 7. Equal ratio coating of Col IV and HA show a regression of growth on day 7.

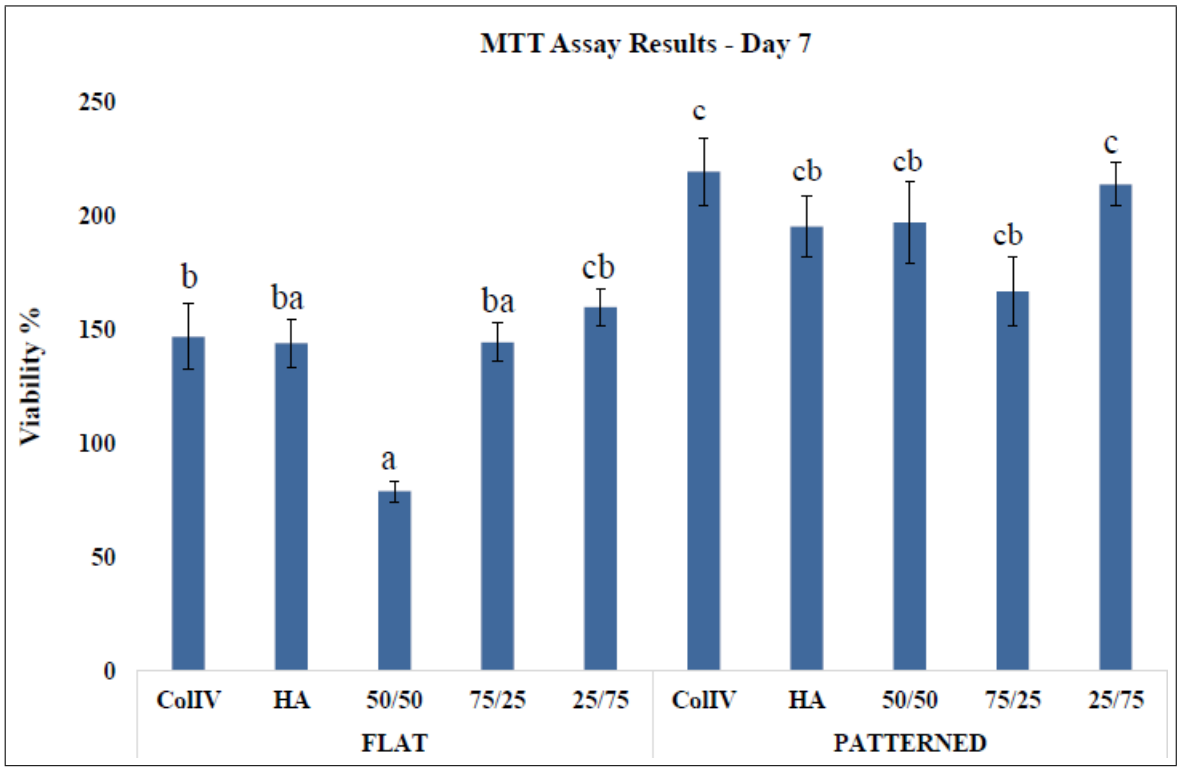

Figure 4.13 MTT assay results at 7^{th} day. Data is expressed in means ± SE ($p < 0{,}05$).

MTT assay results at 1^{st}, 4^{th} and 7^{th} days of culture was shown in Figure 4.14. Patterned substrates outperformed flat substrates in all chemical compositions of coating material. Cell growth continued on all substrates for 7 days regardless of coating or topography of the substrates.

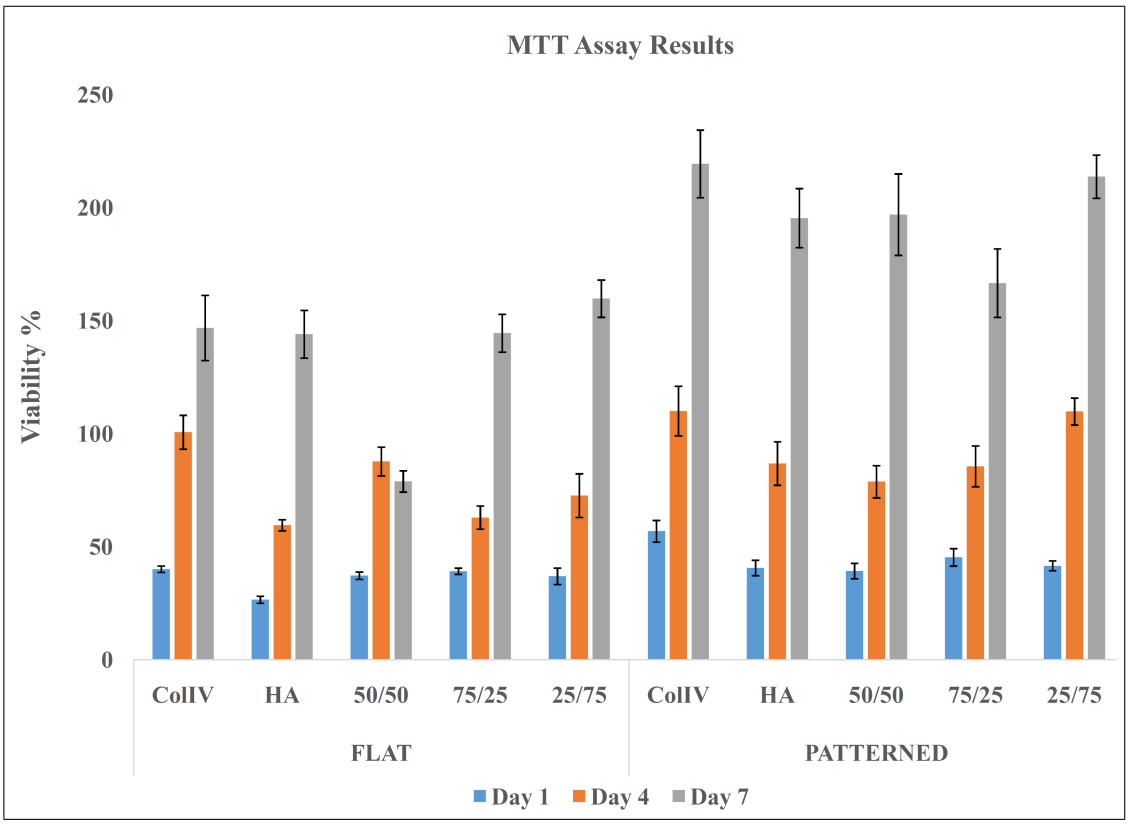

Figure 4.14 MTT assay results at 1^{st}, 4^{th} and 7^{th} days of culture.

4.4.2 F-actin Staining

Images taken from F-actin stained cells on flat PAAm substrates are shown in Figure 4.15. Alexa 488 tagged F-actin filaments of cells are clearly visible in the first column where mixture of equal Col IV and HA shows the most homogenous cell sheet layer formation comparable to TCP. Other coating compositions show mediocre results except for HA coating where cells show smaller morphology. Second column shows DAPI stained cell nuclei where nuclei are distributed homogenously across the substrate in TCP and equal mixture of Col IV and HA coating. Other substrates show heterogeneous distributions due to incomplete cell layer coverage. Merged images are shown in the left column where nuclei can be co-located inside cytoskeletons. Figure 4.16 shows F-actin stained cells on patterned PAAm substrates. Right column shows cytoskeletons of cells where a complete coverage of cell layer is seen in all coating compositions except HA coating. HA coated substrates show smaller cell morphologies similar to flat substrates. DAPI counter-stained cell nuclei show more homogenous distribution compared to flat substrates in all groups except on HA coated substrates. Merged images are shown in the left column where nuclei can be co-located inside cytoskeletons.

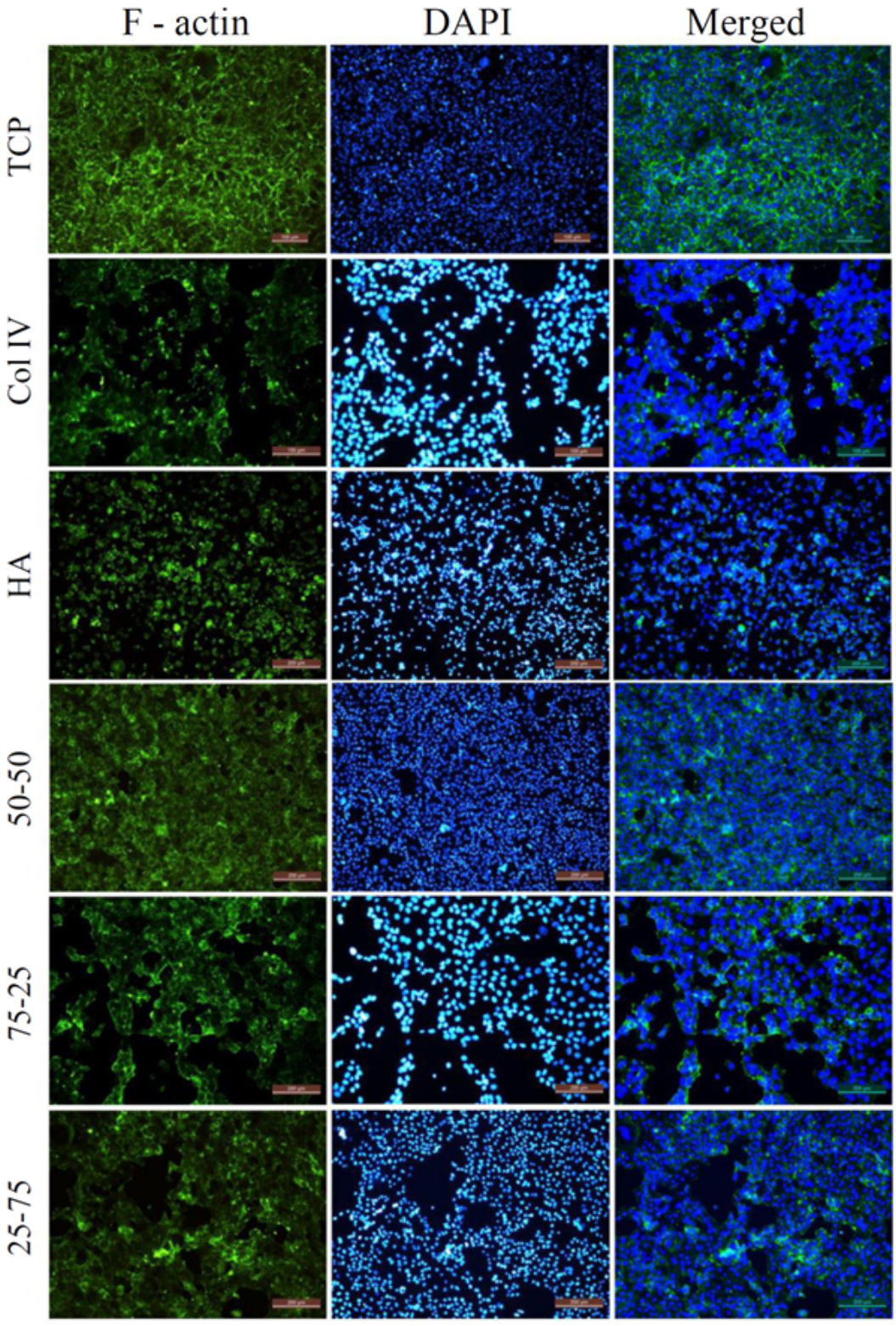

Figure 4.15 F-actin and DAPI staining of Flat Substrates.

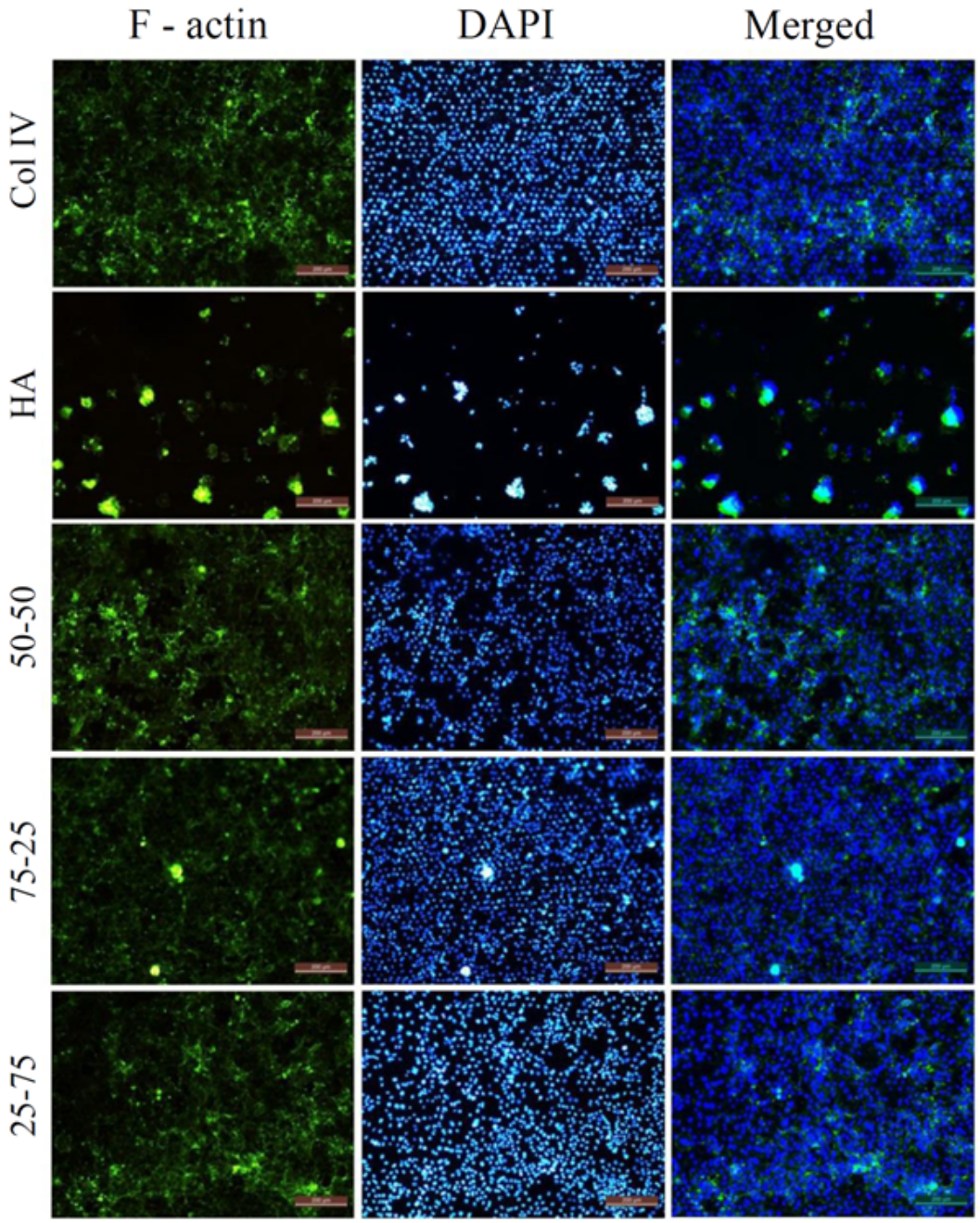

Figure 4.16 F-actin and DAPI staining of Patterned Substrates.

5. DISCUSSION

5.1 Mechanical Characterization

The unreliability of rheometer devices as materials become more elastic and less viscous did not allow characterization of stiff gels with a cross-linker concentration of 0.3%. However softer gels with 0.03% cross-linker concentration gave expected results based on the literature [55]. The fact that G' values are much larger than G" values consistently for all frequencies indicates that samples show close-to-ideal elastic properties. G'/G" ratio which equal tan δ values also show that these values are below 1 indicating elastic gel behavior [62]. Rheometry measurements for stiffer gels on the other hand show wildly varying values in the 0.0-10.0 Hz range. Therefore elastic moduli of these gels were determined by tensile tests. Measured elastic modulus value of around 72 kPa is in agreement with previously reported results of this recipe [52] and within the range of Descemet's membrane elastic modulus value of 20-80 kPa [10].

5.2 Morphological Characterization

Patterns observed in optical microscopy images of PAAm gels has shown that replication was completely successful. Hexagon dimensions exactly fit with designed patterns on silicon wafers. Dimensions of healthy corneal endothelial cells have shown in the literature as 20 μm in diameter and approximately 4 μm in depth [2, 3, 8]. Hexagons inspired from healthy corneal endothelium are 20 μm in diameter which matches optical microscopy images taken from patterned PAAm hydrogels.

5.3 Chemical Characterization

FTIR analysis of plain PAAm gel shows characteristic stretching vibration of amide group at 3191 $cm^{-}1$. Moreover a strong peak at 1651 $cm^{-}1$ was observed due to vibrations of N-H bond of amide group. This peak also has a shoulder at 1612 $cm^{-}1$ which is characteristically attributed to C=O bond of the amide group. The fact that other peaks at 1449 $cm^{-}1$ and 1413 $cm^{-}1$ are in agreement with the literature [63] and absence of any abnormal peaks confidently concludes that PAAm hydrogels are synthesized successfully.

After chemically modifying hydrogels with Col IV and HA using Sulfo-SANPAH method, FTIR analyses show almost identical spectra between these groups and plain gels. This is expected due to the extremely small amount of coating material compared to bulk of the hydrogels. Moreover, coating materials do not contain any chemical bonds with strong IR absorption that is not present in the bulk of PAAm hydrogels. For example upon inspecting chemical structure of HA, it is majorly composed of chemical bonds such as C-H, C-O, C=O, C-O-C and C-C all of which are also present in the bulk of PAAm hydrogels [64]. The only distinguishing bond of HA is O-H bond which has weak and broad IR absorbance that usually gets overpowered by water absorbance at 3300 $cm^{-}1$. The same situation holds true for Col IV as well. In addition to amide bonds between amino acids being abundant in PAAm, chemical bonds within the amino acids do not provide any distinguishing strong IR absorbance peaks either. However a subtle difference was spotted upon close inspection of spectra between 1640 $cm^{-}1$ and 1665 $cm^{-}1$. At 1650 $cm^{-}1$ Col IV shows increased absorbance just enough to change the shape of the spectrum with a downward shoulder. Previous FTIR studies of different collagen types show that Col IV has its highest absorbance within this range [65]. Moreover HA also shows an increased absorbance in this region at 1655 $cm^{-}1$ dominating and completely eliminating the upwards shoulder of plain PAAm in the same wavenumber. HA also has a strong absorption band in this region due to unique environment of its carboxylate groups [66] which completely dominates spectral features of PAAm in this region.

Inconclusive results from FTIR analysis required further investigation in order to confirm presence of coating. Using the concept of immunofluorescence coating materials HA and Col IV were successfully stained using antibodies specific to each one. Using fluorescent tagged secondary antibodies that emit red light for Col IV and green light for HA it was possible to differentially image these molecules covalently bound to PAAm surface. It can be seen in Figure 4.9 that Col IV emits a strong fluorescence signal with the appropriate excitation filter while background signal from substrates treated with only secondary antibodies show a much dimmer signal. This result confirms the presence of covalently bound Col IV on substrate surface. HA coated substrates also show a green fluorescence signal albeit dimmer and comparable to background signal. However upon close inspection of images it is clearly visible that signal from HA moieties on the surface exhibit a much brighter but heterogeneous pattern that is absent on background images. Same phenomenon is also observed on substrates coated with both Col IV and HA. Weak signal from HA coated samples is likely due to lower reactivity of HA in our coating strategy. NHS moiety of sulfo-SANPAH molecule favors coupling with amine groups but also reacts with other nucleophiles. While Col IV presents many amine groups available for coupling reaction, HA only has weak nucleophile groups such as alcohols and carboxylates which less favorable. Since amine groups in Col IV compete for NHS ester of sulfo-SANPAH molecules, the fact that HA signal is even lower in mixture coated substrates is an expected consequence. When Col IV coated samples are excited with blue light or HA coated samples are excited with green light no signal is observed which proves that secondary antibodies do not bind non-selectively since both are applied to all samples.

Results of WCA measurements also confirm the presence of covalently bound coating materials on substrates as contact angle changes greatly between groups. Col IV coated gels become much more hydrophobic in agreement with literature. Contact angle of plain PAAm hydrogels are 33° which is almost exactly the same as previously obtained results in the literature [56]. HA coated gels become more hydrophobic as well but less than Col IV coated samples probably due to extended carbohydrate chain structure of HA chains that interact freely with water. HA also reduce hydrophobicity of Col IV coatings when used in equal ratio due to this reason.

5.4 Cell Culture Studies

Cell viability data obtained from MTT assay gives a first impression about cell behavior on different substrates. As seen in Figure 4.14 presence of hexagonal patterns on substrates increases cell viability on all types of chemical coating composition. This can be attributed to increased surface area of substrates and guidance effect of homogenously distributed troughs which give cells more space to spread out and grow. Cell viability data from flat substrates give the opportunity to evaluate contribution of coating composition independently. In earlier time points other coatings outperform HA coated substrates but cells likely acclimate and start secreting their ECM molecules since they start thriving at day 7. Only equal ratio coating of Col IV and HA show a decrease in cell viability at day 7 which is inexplicable with present data. Future repetitions of this experiment may obliterate this if it's a random deviation. If it persists, other strategies must be utilized to explain this phenomenon. The fact that cell viability increases with time concludes that substrates are non-toxic and biocompatible. Patterned substrates have shown increased viability in all coatings that empowers the argument that deviation in 50/50 coating of flat substrates is random. Coating composition did not cause a significant difference in viability in neither flat nor patterned substrates according to statistical analysis. However increase in viability for patterned substrates was significant according to statistical analysis.

These results are further supplemented by F-actin staining images. Cells on TCP show a homogenous distribution and a decent cell sheet formation. Other groups in flat substrates show that only 25/75 and 50/50 ratio mixtures have comparable performance to TCP. Even though coating material did not create a significant difference in cell viability at day 7, it seems that cell morphology is highly sensitive to this factor. Moreover even though HA coated substrates show increased viability at day 7, these images conclude that they still have poor morphological qualities. Upon inspection of F-actin staining images on patterned substrates the most striking difference was the distribution of DAPI stained cell nuclei. It seems that even though whole cells are not confined to pattern troughs, nuclei are guided towards these crevices. As a result an extremely homogenous distribution of nuclei is obtained. Stained cytoskeletons show

that this distribution causes morphological changes to entire cell as only HA coated substrates failed to form complete cell sheets. Interestingly, patterns seem to aggravate poor performance of HA coatings as these cells show even smaller diameters. The fact that 50/50 mixture of Col IV and HA show an exceptional quality of cell sheet further strengthens the idea that viability decrease of this group at day 7 is a random deviation from normal trend. The fact that presence of bioinspired patterns on substrates enhance cell sheet formation is proven in both F-actin staining images and statistical analysis of MTT assay results.In the literature, there are also several studies to investigate the effect of nano and micro topography of substrates on CECs' behaviors. As an example, a study shows that micron features on the TCP improve the proliferation of HCECs approximately 3-fold while nano-scaled features also improve the polygonal morphology of cells [67]. Other study demonstrates that substrate topography and biochemical cues affects HCECs' behaviors and improve cell morphology and phenotype [6]. In another study in which tested different topographies for BCECs, the following conclusion was reached that suitable geometry and dimensions of substrate topography can be able to improve CECs' response to mimic healthy corneal endothelium [68]. These studies confirm the positive effects of the substrate topography on cell behavior in our study.

It can be speculated that cell nuclei positioning into pattern crevices activate some molecular pathways within the cell that encourages cell sheet formation. Extended studies should be performed in order to pinpoint activated chemical pathways in this phenomenon.

5.5 Future Studies

In this study, the results of cell culture experiments indicated that the surface topography of substrates affects the viability of corneal endothelial cells. In future studies, cell viability experiments will be expanded to 21 days. Moreover, patterns inspired from diseased corneal endothelium will be created on substrates and will be compared to the substrates inspired from healthy corneal endothelium. The amounts of Col IV and HA covalently bound to substrates will be quantified. The cell sheet planned to be obtained would be a promising tool for in vitro drug toxicity tests. Furthermore, other hydrogel types that are suitable for cell sheet detachment can be used within this concept for in vivo applications.

REFERENCES

1. Joyce, N. C., "Proliferative capacity of the corneal endothelium," *Progress in Retinal and Eye Research*, Vol. 22, no. 3, pp. 359–389, 2003.

2. Zavala, J., G. Ló Pez Jaime, C. R. Barrientos, and J. Valdez-Garcia, "Corneal endothelium: developmental strategies for regeneration," *Eye*, Vol. 27, no. January, pp. 579–588, 2013.

3. Bourne, W. M., "Biology of the corneal endothelium in health and disease.," *Eye (London, England)*, Vol. 17, no. 8, pp. 912–8, 2003.

4. Ruberti, J. W., A. S. Roy, and C. J. Roberts, "Corneal biomechanics and biomaterials.," *Annual review of biomedical engineering*, Vol. 13, pp. 269–295, 2011.

5. Bartakova, A., N. J. Kunzevitzky, and J. L. Goldberg, "Regenerative Cell Therapy for Corneal Endothelium," *Current Ophthalmology Reports*, Vol. 2, no. 3, pp. 81–90, 2014.

6. Koo, S., R. Muhammad, G. S. L. Peh, J. S. Mehta, and E. K. F. Yim, "Micro- and nanotopography with extracellular matrix coating modulate human corneal endothelial cell behavior," *Acta Biomaterialia*, Vol. 10, no. 5, pp. 1975–1984, 2014.

7. Palchesko, R. N., K. L. Lathrop, J. L. Funderburgh, and A. W. Feinberg, "In vitro expansion of corneal endothelial cells on biomimetic substrates.," *Scientific reports*, Vol. 5, p. 7955, 2015.

8. Eghrari, A. O., S. A. Riazuddin, and J. D. Gottsch, *Overview of the Cornea: Structure, Function, and Development*, Vol. 134, Elsevier Inc., 1 ed., 2015.

9. Derek W. DelMonte, T. K., "Anatomy and physiology of the cornea and related structures," *J Cataract Refract Surg*, Vol. 37, no. 3, pp. 588–598, 2011.

10. Last, J. A., S. J. Liliensiek, P. F. Nealey, and C. J. Murphy, "Determining the mechanical properties of human corneal basement membranes with atomic force microscopy," *Journal of Structural Biology*, Vol. 167, no. 1, pp. 19–24, 2009.

11. Last, J. A., S. M. Thomasy, C. R. Croasdale, P. Russell, and C. J. Murphy, "Compliance profile of the human cornea as measured by atomic force microscopy.," *Micron (Oxford, England : 1993)*, Vol. 43, no. 12, pp. 1293–8, 2012.

12. Torricelli, A. A. M., V. Singh, M. R. Santhiago, and S. E. Wilson, "The corneal epithelial basement membrane: structure, function, and disease.," *Investigative ophthalmology & visual science*, Vol. 54, no. 9, pp. 6390–400, 2013.

13. Wilson, S. E., and J. W. Hong, "Bowman's layer structure and function: critical or dispensable to corneal function? A hypothesis.," *Cornea*, Vol. 19, no. 4, pp. 417–420, 2000.

14. Joyce, N. C., "Proliferative capacity of corneal endothelial cells," *Experimental Eye Research*, Vol. 95, no. 1, pp. 16–23, 2012.

15. Gambato, C., E. Longhin, A. G. Catania, D. Lazzarini, R. Parrozzani, and E. Midena, "Aging and corneal layers: an in vivo corneal confocal microscopy study," *Graefe's Archive for Clinical and Experimental Ophthalmology*, Vol. 253, no. 2, pp. 267–275, 2014.

16. Fischbarg, J., "The Corneal Endothelium," *The Biology of the Eye*, Vol. Volume 10, no. 05, pp. 113–125, 2005.

17. Luengo-Gimeno, F., D. T. Tan, and J. S. Mehta, "Evolution of deep anterior lamellar keratoplasty (DALK).," *The ocular surface*, Vol. 9, no. 2, pp. 98–110, 2011.

18. Lee, W. B., D. S. Jacobs, D. C. Musch, S. C. Kaufman, W. J. Reinhart, and R. M. Shtein, "Descemet's Stripping Endothelial Keratoplasty: Safety and Outcomes. A Report by the American Academy of Ophthalmology," *Ophthalmology*, Vol. 116, no. 9, pp. 1818–1830, 2009.

19. H Tan, D. T., J. K. G Dart, E. J. Holland, and S. Kinoshita, "Ophthalmology 3 Corneal transplantation," *The Lancet*, Vol. 379, pp. 1749–1761, 2012.

20. Okumura, N., M. Ueno, N. Koizumi, Y. Sakamoto, K. Hirata, J. Hamuro, and S. Kinoshita, "Enhancement on primate corneal endothelial cell survival in vitro by a rock inhibitor," *Investigative Ophthalmology and Visual Science*, Vol. 50, no. 8, pp. 3680–3687, 2009.

21. Lin, G. G.-h., and J. G. Scott, "NIH Public Access," Vol. 100, no. 2, pp. 130–134, 2012.

22. Teichmann, J., M. Valtink, S. Gramm, M. Nitschke, C. Werner, R. H. W. Funk, and K. Engelmann, "Human corneal endothelial cell sheets for transplantation: Thermo-responsive cell culture carriers to meet cell-specific requirements," *Acta Biomaterialia*, Vol. 9, no. 2, pp. 5031–5039, 2013.

23. Moysidis, S. N., K. Alvarez-Delfin, V. J. Peschansky, E. Salero, A. D. Weisman, A. Bartakova, G. A. Raffa, R. M. Merkhofer, K. E. Kador, N. J. Kunzevitzky, and J. L. Goldberg, "Magnetic field-guided cell delivery with nanoparticle-loaded human corneal endothelial cells," *Nanomedicine: Nanotechnology, Biology, and Medicine*, Vol. 11, no. 3, pp. 499–509, 2015.

24. Ishino, Y., Y. Sano, T. Nakamura, C. J. Connon, H. Rigby, N. J. Fullwood, and S. Kinoshita, "Amniotic membrane as a carrier for cultivated human corneal endothelial cell transplantation," *Invest Ophthalmol Vis Sci*, Vol. 45, no. 3, pp. 800–806, 2004.

25. Yoeruek, E., T. Bayyoud, C. Maurus, J. Hofmann, M. S. Spitzer, K. U. Bartz-Schmidt, and P. Szurman, "Decellularization of porcine corneas and repopulation with human corneal cells for tissue-engineered xenografts," *Acta Ophthalmologica*, Vol. 90, no. 2, 2012.

26. Kopsachilis, N., I. Tsinopoulos, T. Tourtas, F. E. Kruse, and U. W. Luessen, "Descemet's membrane substrate from human donor lens anterior capsule," *Clinical and Experimental Ophthalmology*, Vol. 40, no. 2, pp. 187–194, 2012.

27. Navaratnam, J., T. Utheim, V. Rajasekhar, and A. Shahdadfar, "Substrates for Expansion of Corneal Endothelial Cells towards Bioengineering of Human Corneal Endothelium," *Journal of Functional Biomaterials*, Vol. 6, no. 3, pp. 917–945, 2015.

28. Choi, J. S., E. Y. Kim, M. J. Kim, M. Giegengack, F. a. Khan, G. Khang, and S. Soker, "In vitro evaluation of the interactions between human corneal endothelial cells and extracellular matrix proteins.," *Biomedical materials (Bristol, England)*, Vol. 8, no. 1, p. 014108, 2013.

29. Watanabe, R., R. Hayashi, Y. Kimura, Y. Tanaka, T. Kageyama, S. Hara, Y. Tabata, and K. Nishida, "A novel gelatin hydrogel carrier sheet for corneal endothelial transplantation.," *Tissue engineering. Part A*, Vol. 17, pp. 2213–2219, 2011.

30. Levis, H. J., G. S. L. Peh, K. P. Toh, R. Poh, A. J. Shortt, R. A. L. Drake, J. S. Mehta, and J. T. Daniels, "Plastic Compressed Collagen as a Novel Carrier for Expanded Human Corneal Endothelial Cells for Transplantation," *PLoS ONE*, Vol. 7, no. 11, 2012.

31. Liang, Y., W. Liu, B. Han, C. Yang, Q. Ma, W. Zhao, M. Rong, and H. Li, "Fabrication and characters of a corneal endothelial cells scaffold based on chitosan," *Journal of Materials Science: Materials in Medicine*, Vol. 22, no. 1, pp. 175–183, 2011.

32. Ozcelik, B., K. D. Brown, A. Blencowe, M. Daniell, G. W. Stevens, and G. G. Qiao, "Ultrathin chitosan-poly(ethylene glycol) hydrogel films for corneal tissue engineering," *Acta Biomaterialia*, Vol. 9, no. 5, pp. 6594–6605, 2013.

33. Hadlock, T., S. Singh, J. P. Vacanti, and B. J. McLaughlin, "Ocular cell monolayers cultured on biodegradable substrates.," *Tissue engineering*, Vol. 5, no. 3, pp. 187–96, 1999.

34. Lai, J.-Y., K.-H. Chen, and G.-H. Hsiue, "Tissue-engineered human corneal endothelial cell sheet transplantation in a rabbit model using functional biomaterials.," *Transplantation*, Vol. 84, no. 10, pp. 1222–32, 2007.

35. Sanchez, C., H. Arribart, and M. M. Giraud Guille, "Biomimetism and bioinspiration as tools for the design of innovative materials and systems," *Nature Materials*, Vol. 4, no. 4, pp. 277–288, 2005.

36. Theocharis, A. D., S. S. Skandalis, C. Gialeli, and N. K. Karamanos, "Extracellular matrix structure," 2016.

37. Wang, L., and R. L. Carrier, "Biomimetic Topography : Bioinspired Cell Culture Substrates and Scaffolds," *Biomimetic Topography: Bioinspired Cell Culture Substrates and Scaffolds, Advances in Biomimetics*, pp. 453–472, 2011.

38. Bettinger, C. J., R. Langer, and J. T. Borenstein, "Engineering Substrate Micro- and Nanotopography to Control Cell Function," *Angewandte Chemie (International ed. in English)*, Vol. 48, no. 30, pp. 5406–5415, 2009.

39. Discher, D. E., P. Janmey, and Y.-L. Wang, "Tissue cells feel and respond to the stiffness of their substrate.," *Science (New York, N.Y.)*, Vol. 310, no. 5751, pp. 1139–43, 2005.

40. Flemming, R., C. Murphy, G. Abrams, S. Goodman, and P. Nealey, "Effects of synthetic micro-and nano-structured surfaces on cell behavior," *Biomaterials*, Vol. 20, no. 1999, pp. 573–588, 1999.

41. Engler, A. J., S. Sen, H. L. Sweeney, and D. E. Discher, "Matrix Elasticity Directs Stem Cell Lineage Specification," *Cell*, Vol. 126, no. 4, pp. 677–689, 2006.

42. Molladavoodi, S., H.-J. Kwon, J. Medley, and M. Gorbet, "Human corneal epithelial cell response to substrate stiffness.," *Acta biomaterialia*, Vol. 11, pp. 324–32, 2015.

43. Lai, J. Y., and I. H. Tu, "Adhesion, phenotypic expression, and biosynthetic capacity of corneal keratocytes on surfaces coated with hyaluronic acid of different molecular weights," *Acta Biomaterialia*, Vol. 8, no. 3, pp. 1068–1079, 2012.

44. Lai, J.-Y., D. H.-K. Ma, H.-Y. Cheng, C.-C. Sun, S.-J. Huang, Y.-T. Li, and G.-H. Hsiue, "Ocular biocompatibility of carbodiimide cross-linked hyaluronic acid hydrogels for cell sheet delivery carriers.," *Journal of biomaterials science. Polymer edition*, Vol. 21, no. 3, pp. 359–76, 2010.

45. Lai, J. Y., H. Y. Cheng, and D. Hui-Kang Ma, "Investigation of overrun-processed porous hyaluronic acid carriers in corneal endothelial tissue engineering," *PLoS ONE*, Vol. 10, no. 8, 2015.

46. Naghash, H. J., and O. Okay, "Formation and structure of polyacrylamide gels," *Journal of Applied Polymer Science*, Vol. 60, no. 7, pp. 971–979, 1996.

47. Pelham, R. J., and Y.-l. Wang, "Cell locomotion and focal adhesions are regulated by substrate flexibility," *Proceedings of the National Academy of Sciences*, Vol. 94, no. 25, pp. 13661–13665, 1997.

48. Aratyn-Schaus, Y., P. W. Oakes, J. Stricker, S. P. Winter, and M. L. Gardel, "Preparation of complaint matrices for quantifying cellular contraction.," *Journal of visualized experiments : JoVE*, no. 46, pp. 1–6, 2010.

49. Jacot, J. G., A. D. McCulloch, and J. H. Omens, "Substrate stiffness affects the functional maturation of neonatal rat ventricular myocytes.," *Biophysical journal*, Vol. 95, no. 7, pp. 3479–87, 2008.

50. Beningo, K. A., C. M. Lo, and Y. L. Wang, "Flexible polyacrylamide substrata for the analysis of mechanical interactions at cell-substratum adhesions," 2002.

51. Cretu, A., P. Castagnino, and R. Assoian, "Studying the effects of matrix stiffness on cellular function using acrylamide-based hydrogels.," *Journal of visualized experiments : JoVE*, no. 42, pp. 7–11, 2010.

52. Chen, J. H., W. L. K. Chen, K. L. Sider, C. Y. Y. Yip, and C. A. Simmons, "Beta-Catenin Mediates Mechanically Regulated, Transforming Growth Factor-Beta1-Induced Myofibroblast Differentiation of Aortic Valve Interstitial Cells," *Arteriosclerosis, Thrombosis, and Vascular Biology*, Vol. 31, no. 3, pp. 590–597, 2011.

53. Heras-Bautista, C. O., A. Katsen-Globa, N. E. Schloerer, S. Dieluweit, O. M. Abd El Aziz, G. Peinkofer, W. A. Attia, M. Khalil, K. Brockmeier, J. Hescheler, and K. Pfannkuche, "The influence of physiological matrix conditions on permanent culture of induced pluripotent stem cell-derived cardiomyocytes," *Biomaterials*, Vol. 35, no. 26, pp. 7374–7385, 2014.

54. Oyen, M. L., "Mechanical characterisation of hydrogel materials," *International Materials Reviews*, Vol. 59, no. 1, pp. 44–59, 2014.

55. Abidine, Y., V. M. Laurent, R. Michel, A. Duperray, L. I. Palade, and C. Verdier, "Physical properties of polyacrylamide gels probed by AFM and rheology," *EPL (Europhysics Letters)*, Vol. 109, no. 3, p. 38003, 2015.

56. Lanniel, M., E. Huq, S. Allen, L. Buttery, P. M. Williams, and M. R. Alexander, "Substrate induced differentiation of human mesenchymal stem cells on hydrogels with modified surface chemistry and controlled modulus," *Soft Matter*, Vol. 7, no. 14, p. 6501, 2011.

57. Karadag, E., D. Saraydin, S. Cetinkaya, and O. Guven, "In vitro swelling studies and preliminary biocompatibility evaluation of acrylamide-based hydrogels," *Biomaterials*, Vol. 17, no. 1, pp. 67–70, 1996.

58. Trappmann, B., J. E. Gautrot, J. T. Connelly, D. G. T. Strange, Y. Li, M. L. Oyen, M. a. Cohen Stuart, H. Boehm, B. Li, V. Vogel, J. P. Spatz, F. M. Watt, and W. T. S. Huck, "Extracellular-matrix tethering regulates stem-cell fate," *Nature Materials*, Vol. 11, no. 8, pp. 742–742, 2012.

59. Gospodarowicz, D., A. L. Mescher, and C. R. Birdwell, "Stimulation of corneal endothelial cell proliferation in vitro by fibroblast and epidermal growth factors," *Experimental eye research*, Vol. 25, no. 1, pp. 75–89, 1977.

60. Bethea, C. L., and S. L. Kozak, "Effect of extracellular matrix on pc 12 cell shape and dopamine processing," *Molecular and cellular endocrinology*, Vol. 37, no. 3, pp. 319–329, 1984.

61. Wang, T. J., I. J. Wang, S. Chen, Y. H. Chen, and T. H. Young, "The phenotypic response of bovine corneal endothelial cells on chitosan/polycaprolactone blends," *Colloids and Surfaces B: Biointerfaces*, Vol. 90, no. 1, pp. 236–243, 2012.

62. Grattoni, C. a., H. H. Al-Sharji, C. Yang, A. H. Muggeridge, and R. W. Zimmerman, "Rheology and Permeability of Crosslinked Polyacrylamide Gel.," *Journal of colloid and interface science*, Vol. 240, no. 2, pp. 601–607, 2001.

63. Saber-Samandari, S., H. O. Gulcan, S. Saber-Samandari, and M. Gazi, "Efficient removal of anionic and cationic dyes from an aqueous solution using pullulan-graft-polyacrylamide porous hydrogel," *Water, Air, and Soil Pollution*, Vol. 225, no. 11, 2014.

64. Fan, D., B. Wu, Z. Xu, and Q. Gu, "Determination of hyaluronan by spectroscopic methods," *Journal Wuhan University of Technology, Materials Science Edition*, Vol. 21, no. 3, pp. 32–34, 2006.

65. Belbachir, K., R. Noreen, G. Gouspillou, and C. Petibois, "Collagen types analysis and differentiation by FTIR spectroscopy," *Analytical and Bioanalytical Chemistry*, Vol. 395, no. 3, pp. 829–837, 2009.

66. Domingues, R. M. A., M. Silva, P. Gershovich, S. Betta, P. Babo, S. G. Caridade, J. F. Mano, A. Motta, R. L. Reis, and M. E. Gomes, "Development of Injectable Hyaluronic Acid/Cellulose Nanocrystals Bionanocomposite Hydrogels for Tissue Engineering Applications," *Bioconjugate Chemistry*, Vol. 26, no. 8, pp. 1571–1581, 2015.

67. Muhammad, R., G. S. L. Peh, K. Adnan, J. B. K. Law, J. S. Mehta, and E. K. F. Yim, "Micro- and nano-topography to enhance proliferation and sustain functional markers of donor-derived primary human corneal endothelial cells," *Acta Biomaterialia*, Vol. 19, pp. 138–148, 2015.

68. Teo, B. K. K., K. J. Goh, Z. J. Ng, S. Koo, and E. K. F. Yim, "Functional reconstruction of corneal endothelium using nanotopography for tissue-engineering applications," *Acta Biomaterialia*, Vol. 8, no. 8, pp. 2941–2952, 2012.